

Modeling Sea Ice *in a changing climate*

Kenneth M. Golden
Department of Mathematics
University of Utah



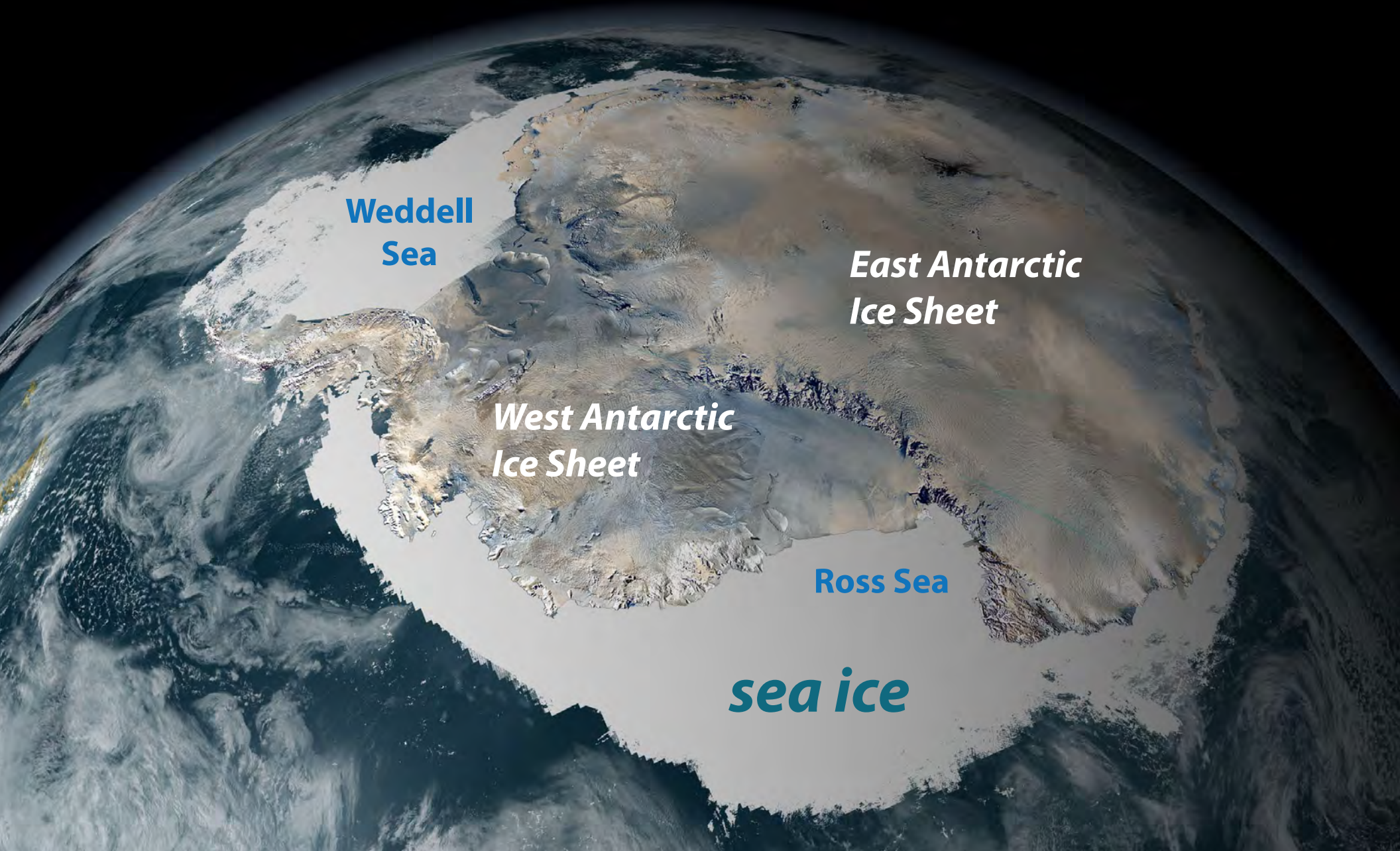
*Alison Kohout
September 2012*

**Workshop on Applied Mathematics
Stanford University**

In Memory of Joseph B. Keller
20 May 2017

ANTARCTICA

southern cryosphere



**Weddell
Sea**

***East Antarctic
Ice Sheet***

***West Antarctic
Ice Sheet***

Ross Sea

sea ice

SEA ICE covers 7 - 10% of earth's ocean surface

- boundary between ocean and atmosphere
- mediates exchange of heat, gases, momentum
- global ocean circulation
- indicator and agent of **climate change**



polar ice caps critical to global climate in reflecting incoming solar radiation



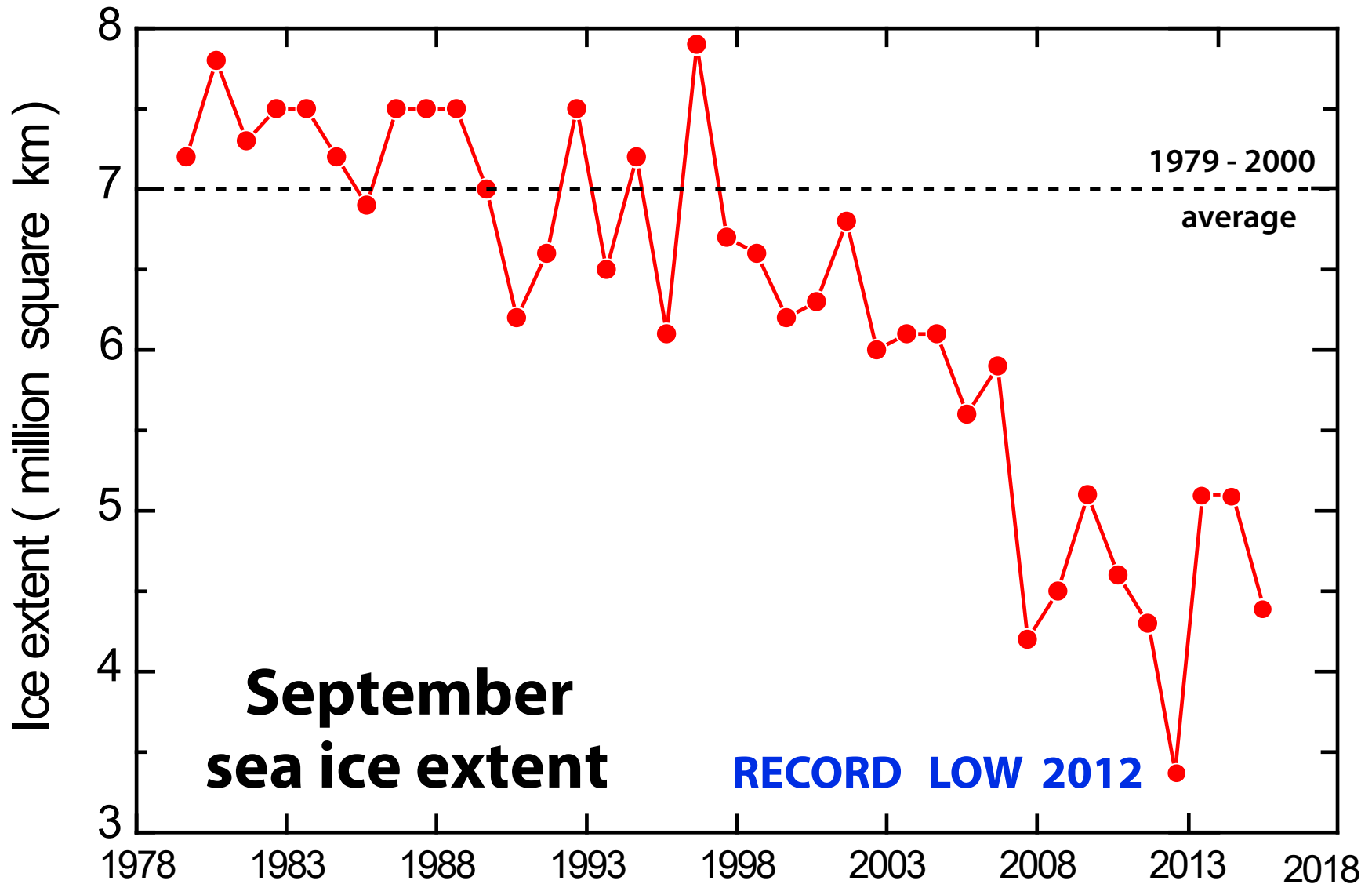
white snow and ice
reflect



dark water and land
absorb

$$\text{albedo } \alpha = \frac{\text{reflected sunlight}}{\text{incident sunlight}}$$

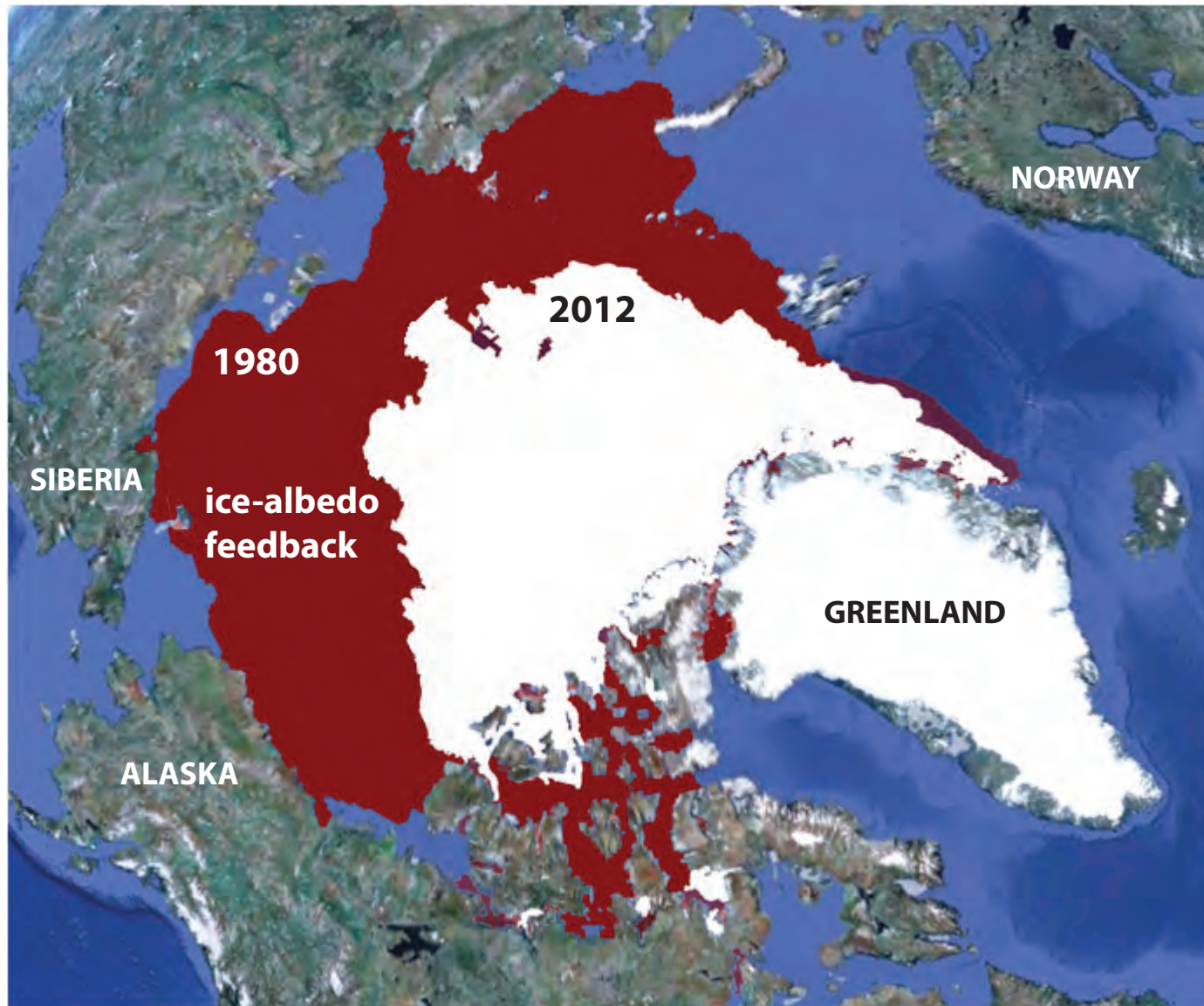
the summer Arctic sea ice pack is melting



Change in Arctic Sea Ice Extent

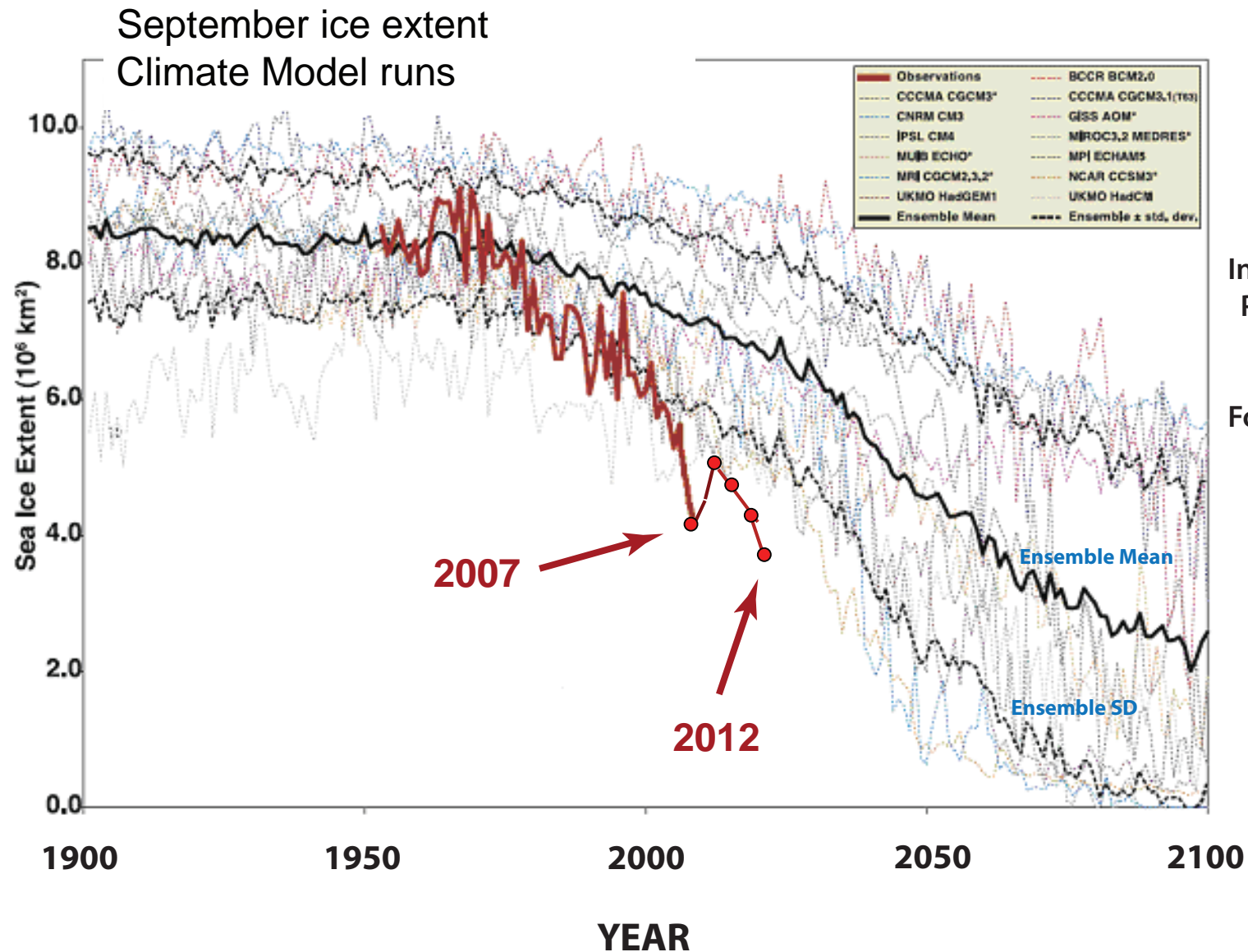
September 1980 -- **7.8** million square kilometers

September 2012 -- **3.4** million square kilometers



Arctic sea ice decline - faster than predicted by climate models

Stroeve et al., GRL, 2007



**IPCC AR4
Models**

Intergovernmental
Panel on Climate
Change (IPCC)

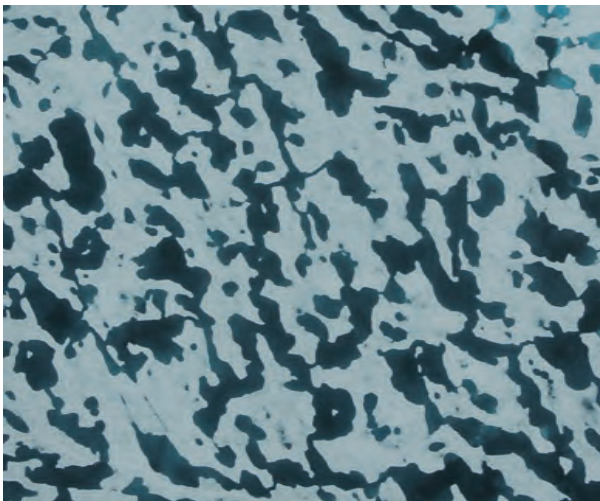
Fourth Assessment
AR4, 2007

challenge

represent sea ice more rigorously in climate models

account for key processes

such as melt pond evolution



Impact of melt ponds on Arctic sea ice
simulations from 1990 to 2007

Flocco, Schroeder, Feltham, Hunke, *JGR Oceans* 2012

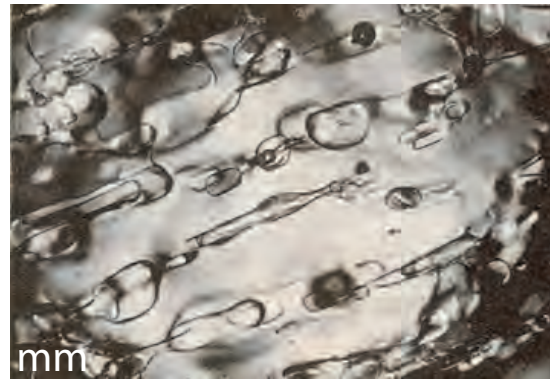
**For simulations with ponds
September ice volume is nearly 40% lower.**

... and other sub-grid scale structures and processes

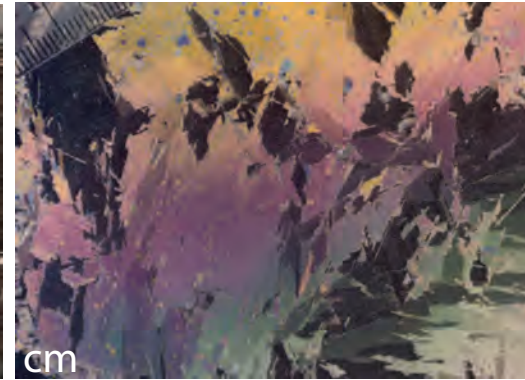
linkage of scales

sea ice is a multiscale composite
displaying structure over 10 orders of magnitude

0.1 millimeter



brine inclusions



polycrystals



horizontal

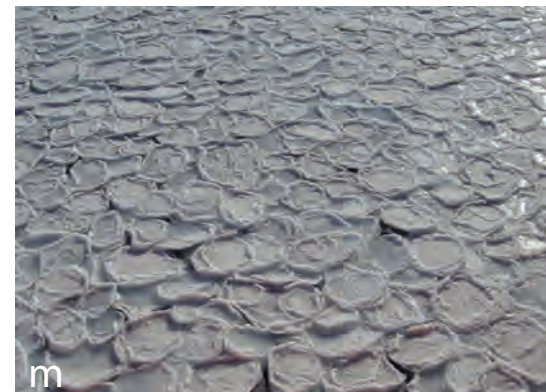


brine channels



vertical

1 meter

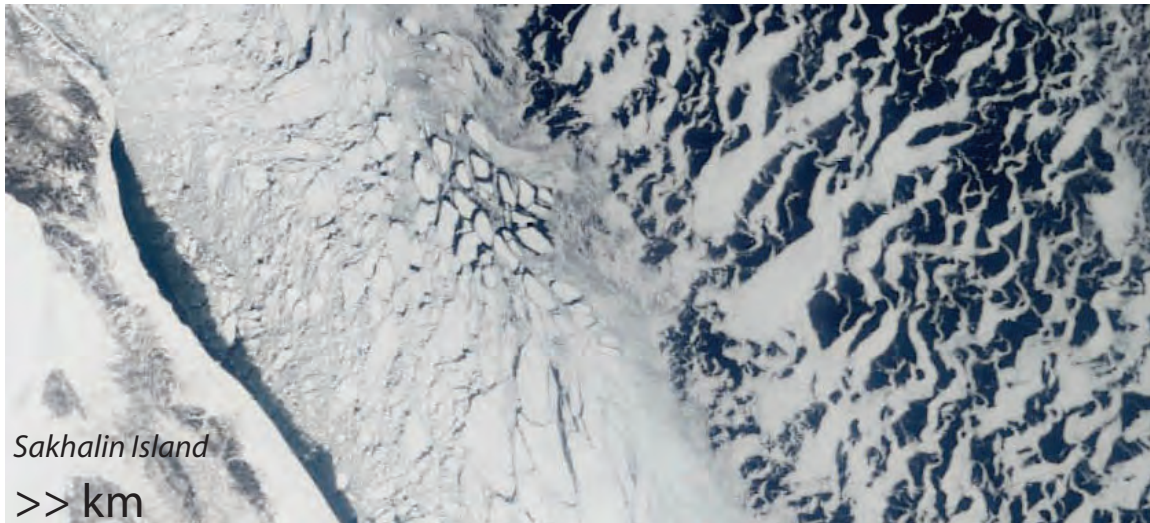


pancake ice

1 meter



100 kilometers



What is this talk about?

Using the mathematics of composite materials and statistical physics to study sea ice structures and processes ... to improve projections of climate change.

... and a brief tour through some of Joe's work!

1. Climate modeling and the polar ice packs

partial differential equations, stochastic differential equations

2. Sea ice microphysics and composite structure

homogenization, fluid flow, diffusion processes, percolation theory

3. EM monitoring of sea ice

homogenization, integral representations, random matrix theory

4. Advection diffusion; polycrystals; waves in the MIZ

homogenization, integral representations, bounds

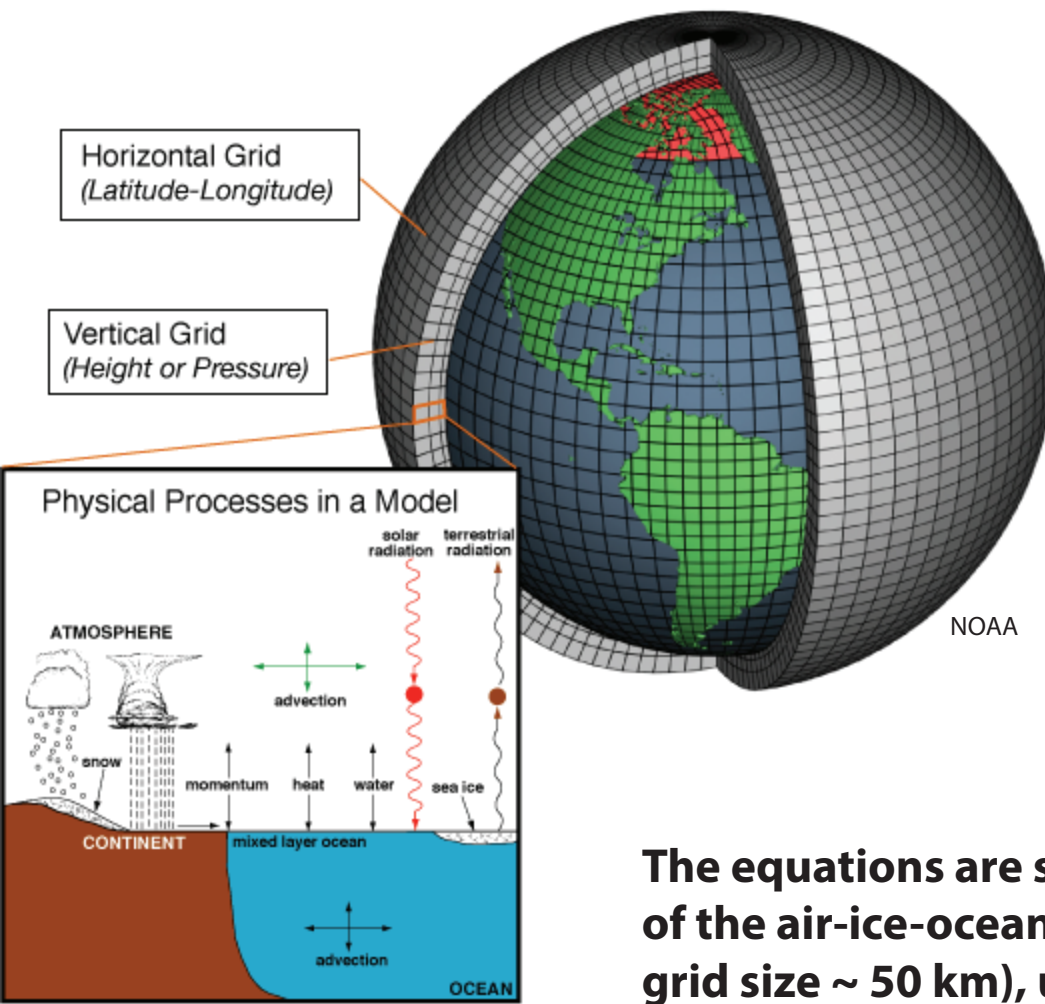
5. Evolution of Arctic melt ponds, fractal geometry

continuum percolation, network and Ising models

critical behavior

cross - pollination

Global Climate Models



Climate models are systems of partial differential equations (PDE) derived from the basic laws of physics, chemistry, and fluid motion.

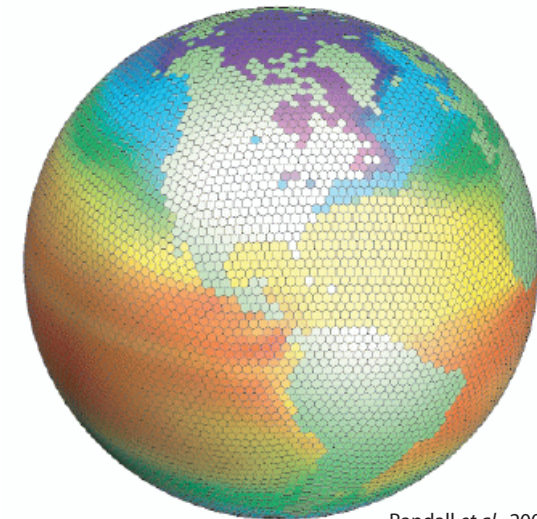
They describe the state of the ocean, ice, atmosphere, land, and their interactions.

The equations are solved on 3-dimensional grids of the air-ice-ocean-land system (with horizontal grid size ~ 50 km), using very powerful computers.

key challenge :

incorporating sub - grid scale processes

linkage of scales



sea ice components of GCM's

What are the key ingredients -- or **governing equations** that need to be solved on grids using powerful computers?

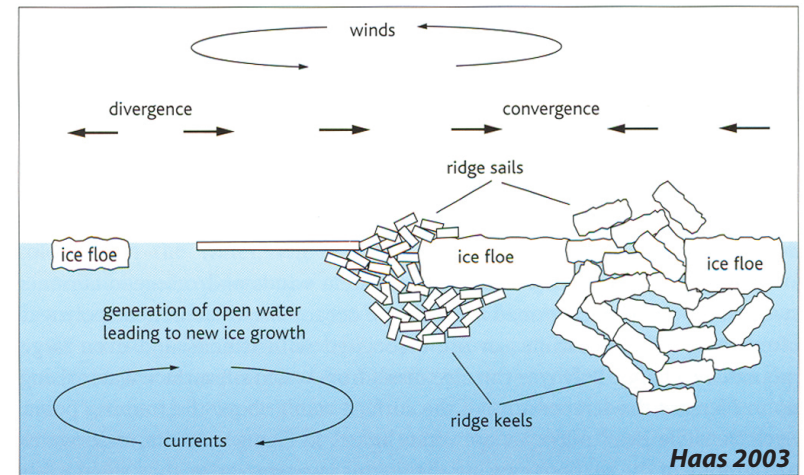
1. Ice thickness distribution $g(x, y, h, t)$ evolution equation **dynamics** + **thermodynamics**
(Thorndike et al. 1975)

$$\frac{Dg}{Dt} = -g \nabla \cdot \mathbf{u} + \Psi(g) - \frac{\partial}{\partial h} (\tau g) + \mathcal{L}$$

**nonlinear PDE with
ice velocity field**

**ice growth
ice melting**

**mechanical redistribution
- ridging and opening**



2. Conservation of momentum, stress vs. strain relation (Hibler 1979)

$$m \frac{D\mathbf{u}}{Dt} = -m f \mathbf{k} \times \mathbf{u} + \boldsymbol{\tau}_a + \boldsymbol{\tau}_o - mg \nabla H + \mathbf{F}_{int} \quad \mathbf{F} = m\mathbf{a} \text{ for sea ice dynamics}$$

3. Heat equation of sea ice and snow

(Maykut and Untersteiner 1971)

$$\frac{\partial T}{\partial t} + \mathbf{u}_{br} \cdot \nabla T = \nabla \cdot k(T) \nabla T$$

thermodynamics

**+ balance of radiative and
thermal fluxes on interfaces**

transform ice thickness distribution equation to Fokker-Planck type equation; Boltzmann framework

Toppaladoddi and Wettlaufer, *PRL*, 2015

thickness h is a diffusion process with probability density $g(h,t)$

“microscopic” mechanical processes that influence ice thickness distribution—rafting, ridging, and open water formation occur over very rapid time scales relative to geophysical-scale changes of $g(h)$

$$\Psi = \int_0^\infty [g(h+h')w(h+h',h') - g(h)w(h,h')]dh' \quad w = \text{transition probability}$$

moments k_1, k_2

Fokker-Planck

$$\frac{\partial g}{\partial t} = -\frac{\partial}{\partial h} \left[\left(\frac{\epsilon}{h} - k_1 \right) g \right] + \frac{\partial^2}{\partial h^2} (k_2 g)$$

Langevin

$$\frac{dh}{dt} = \left(\frac{\epsilon}{h} - k_1 \right) + \sqrt{2k_2} \xi(t) \quad \xi(t) = \text{Gaussian white noise}$$

sea ice microphysics

fluid transport

fluid flow through the porous microstructure of sea ice governs key processes in polar climate and ecosystems

evolution of Arctic melt ponds and sea ice albedo



nutrient flux for algal communities



T. Maksym and T. Markus, 2008

*Antarctic surface flooding
and snow-ice formation*

September
snow-ice
estimates

- *evolution of salinity profiles*
- *ocean-ice-air exchanges of heat, CO₂*

sea ice ecosystem



sea ice algae
support life in the polar oceans

fluid permeability k of a porous medium

porous
concrete



how much water
gets through the
sample per unit
time?

HOMOGENIZATION

mathematics for analyzing effective behavior of heterogeneous systems

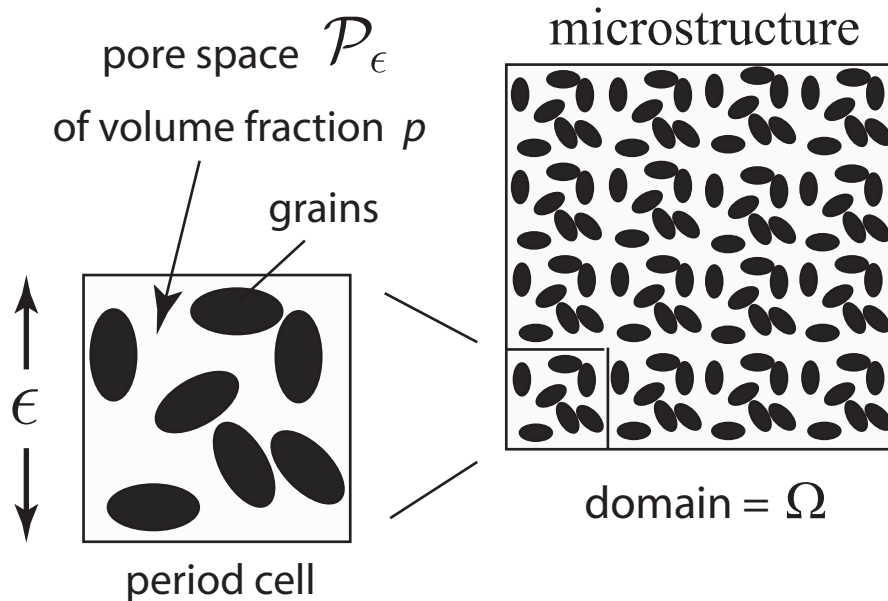
Random media

Joseph B. Keller

- 1964 F. Karal and J. B. Keller, *J. Math. Phys.*
Elastic, Electromagnetic, and Other Waves in a Random Medium
- 1979 J. B. Keller, *Mathematics of Wave Propagation in Random Media*
- 1980 J. B. Keller, *Nonlinear PDE in Engineering and Applied Science*
Darcy's law for flow in porous media and the two-space method
- 1991 R. Burridge and J. B. Keller, *J. Acoustical. Soc. Amer.*
Poroelasticity equations derived from microstructure
- 2001 J. B. Keller, *Transport in Porous Media*
Flow in random porous media

HOMOGENIZE as $\epsilon \rightarrow 0$

Stokes equations for fluid velocity \mathbf{v}^ϵ , pressure p^ϵ , force \mathbf{f} :



$$\nabla p^\epsilon - \epsilon^2 \eta \Delta \mathbf{v}^\epsilon = \mathbf{f}, \quad x \in \mathcal{P}_\epsilon$$

$$\nabla \cdot \mathbf{v}^\epsilon = 0, \quad x \in \mathcal{P}_\epsilon$$

$$\mathbf{v}^\epsilon = 0, \quad x \in \partial \mathcal{P}_\epsilon$$

η = fluid viscosity

via two-scale expansion

MACROSCOPIC EQUATIONS $\mathbf{v}^\epsilon \rightarrow \mathbf{v}$, $p^\epsilon \rightarrow p$ as $\epsilon \rightarrow 0$

Darcy's law $\mathbf{v} = -\frac{1}{\eta} \mathbf{k} \nabla p, \quad x \in \Omega$ $\mathbf{k}(x)$ = effective fluid permeability tensor

($\mathbf{f} = 0$) $\nabla \cdot \mathbf{v} = 0, \quad x \in \Omega$

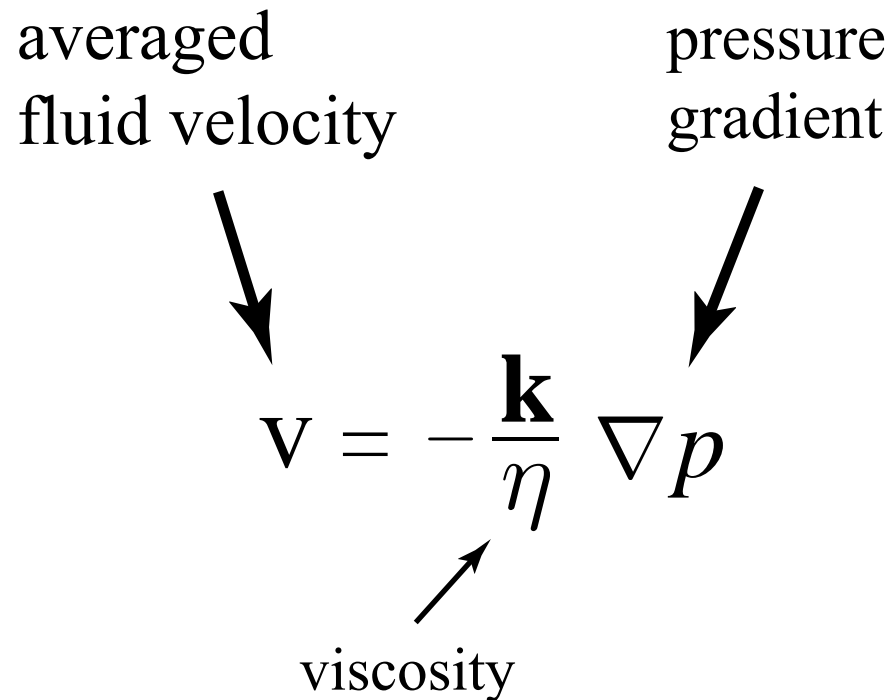
Darcy's Law for slow viscous flow in a porous medium

averaged
fluid velocity

pressure
gradient

$$\mathbf{v} = -\frac{\mathbf{k}}{\eta} \nabla p$$

viscosity

The diagram shows the equation $\mathbf{v} = -\frac{\mathbf{k}}{\eta} \nabla p$ centered on the slide. Three labels with arrows point to parts of the equation: 'averaged fluid velocity' points to \mathbf{v} , 'pressure gradient' points to ∇p , and 'viscosity' points to η .

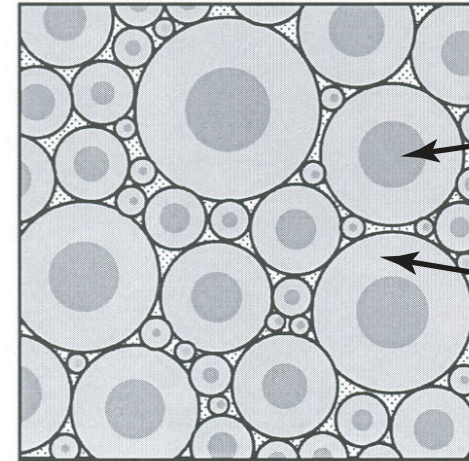
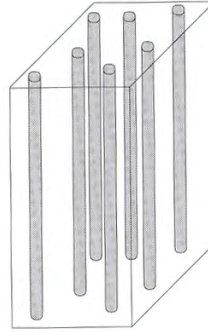
\mathbf{k} = fluid permeability tensor

PIPE BOUNDS on vertical fluid permeability k

Golden, Heaton, Eicken, Lytle, Mech. Materials 2006

Golden, Eicken, Heaton, Miner, Pringle, Zhu, Geophys. Res. Lett. 2007

vertical pipes
with appropriate radii
maximize k



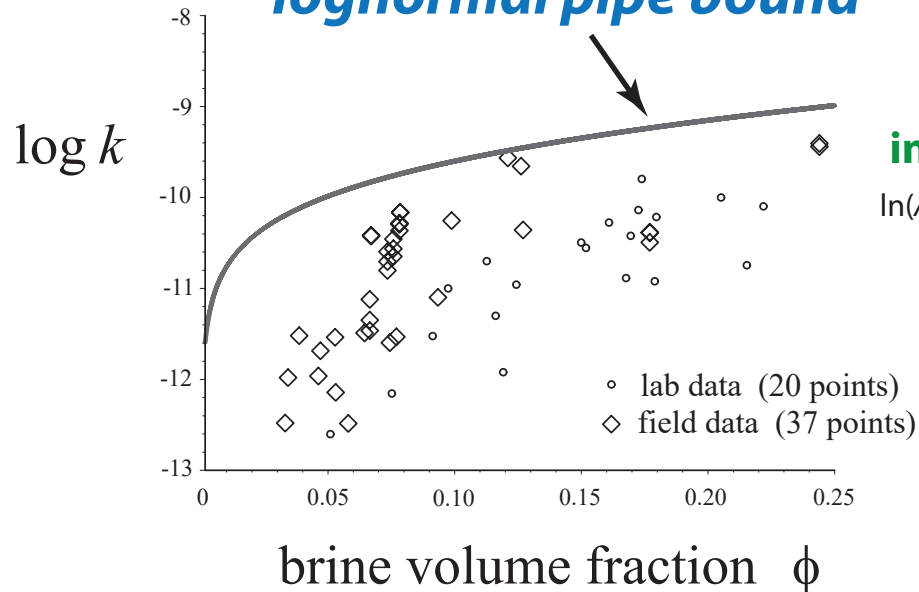
brine

ice

optimal coated
cylinder geometry

fluid analog of arithmetic mean upper bound for effective conductivity of composites (Wiener 1912)

lognormal pipe bound



Golden et al., Geophys. Res. Lett. 2007

$$k \leq \frac{\phi \langle R^4 \rangle}{8 \langle R^2 \rangle} = \frac{\phi}{8} \langle R^2 \rangle e^{\sigma^2}$$

inclusion cross sectional areas A lognormally distributed

$\ln(A)$ normally distributed, mean μ (increases with T) variance σ^2 (Gow and Perovich 96)

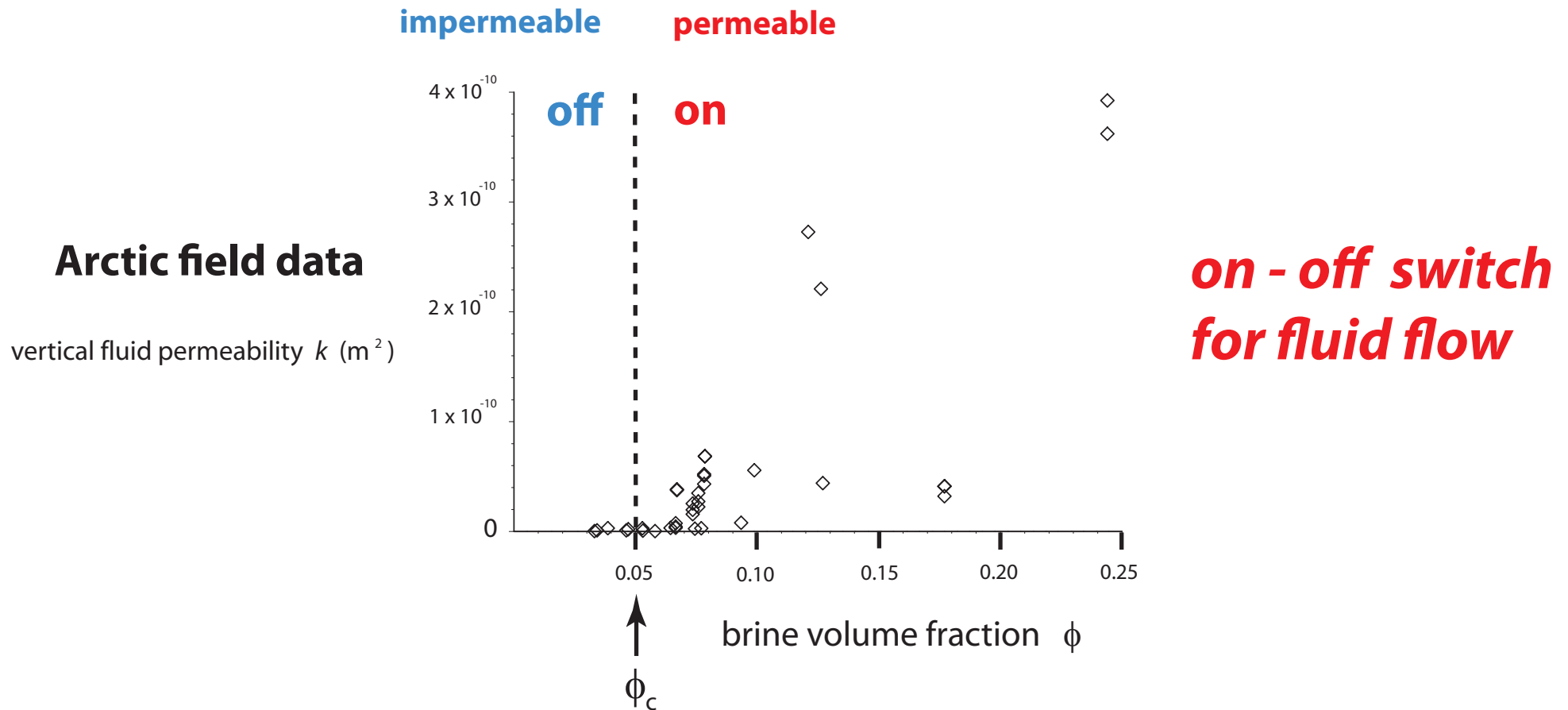
get bounds through variational analysis of
trapping constant γ for diffusion process
in pore space with absorbing BC

Torquato and Pham, PRL 2004

$$\mathbf{k} \leq \gamma^{-1} \mathbf{I}$$

for any ergodic porous medium
(Torquato 2002, 2004)

Critical behavior of fluid transport in sea ice



critical brine volume fraction $\phi_c \approx 5\%$ \longleftrightarrow $T_c \approx -5^\circ \text{C}$, $S \approx 5 \text{ ppt}$

RULE OF FIVES

Golden, Ackley, Lytle *Science* 1998

Golden, Eicken, Heaton, Miner, Pringle, Zhu, *Geophys. Res. Lett.* 2007

Pringle, Miner, Eicken, Golden *J. Geophys. Res.* 2009



sea ice algal communities

D. Thomas 2004

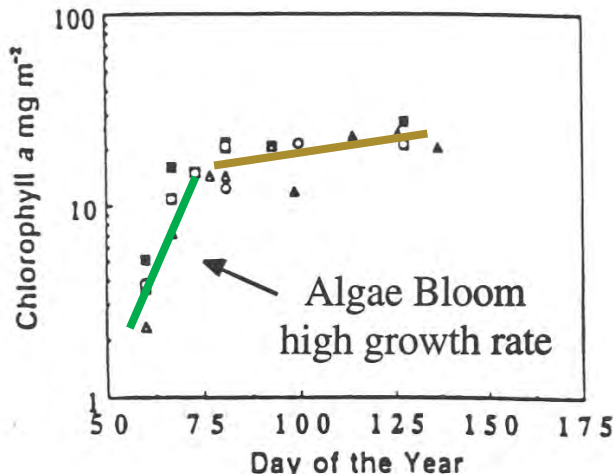
nutrient replenishment
controlled by ice permeability

biological activity turns on
or off according to
rule of fives

Golden, Ackley, Lytle Science 1998

Fritsen, Lytle, Ackley, Sullivan Science 1994

critical behavior of microbial activity

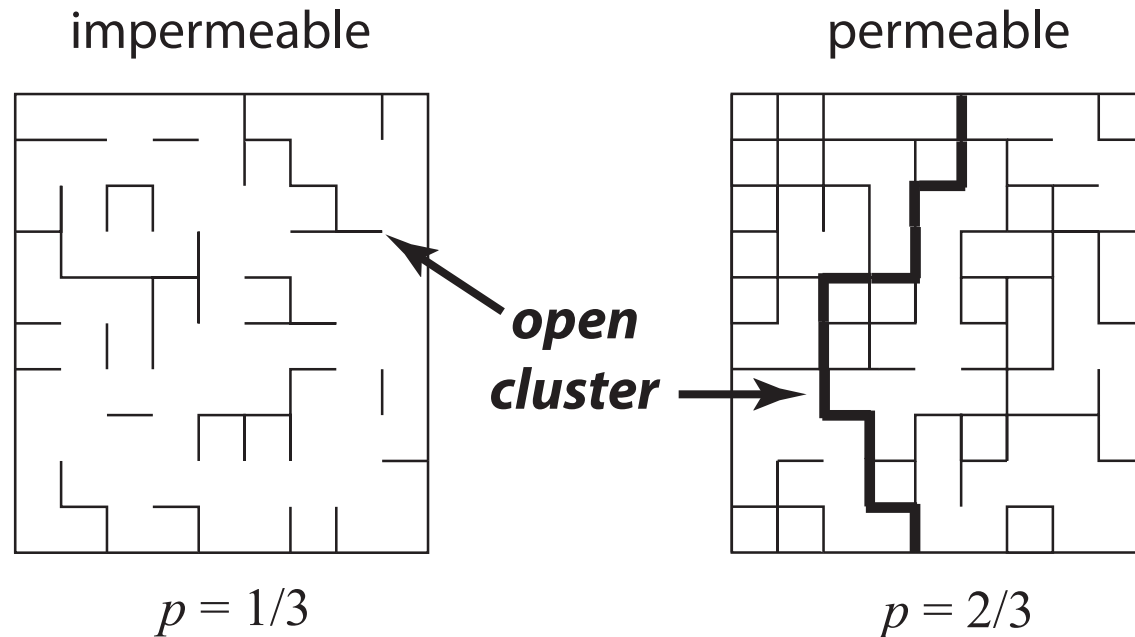


Convection-fueled algae bloom
Ice Station Weddell

Why is the rule of fives true?

percolation theory

probabilistic theory of connectedness



bond \longrightarrow **open** with probability p
closed with probability $1-p$

percolation threshold

$$p_c = 1/2 \quad \text{for } d = 2$$

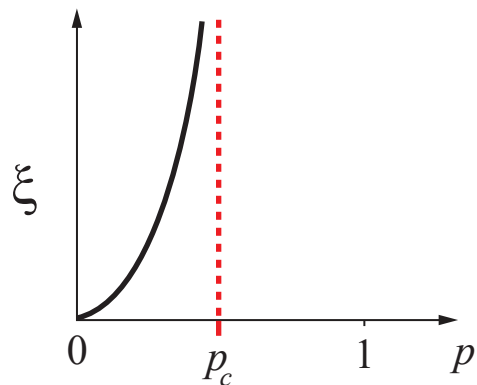
smallest p for which there is an infinite open cluster

order parameters in percolation theory

geometry

correlation length

characteristic scale
of connectedness

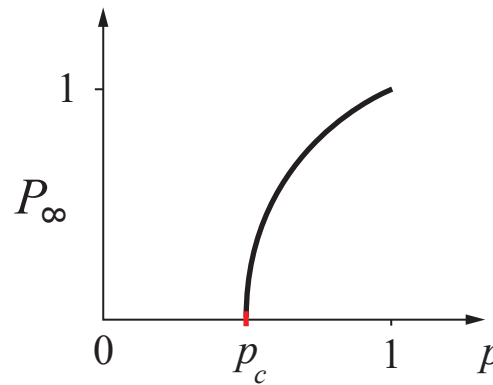


$$\xi(p) \sim |p - p_c|^{-\nu}$$

$$p \rightarrow p_c$$

infinite cluster density

probability the origin
belongs to infinite cluster

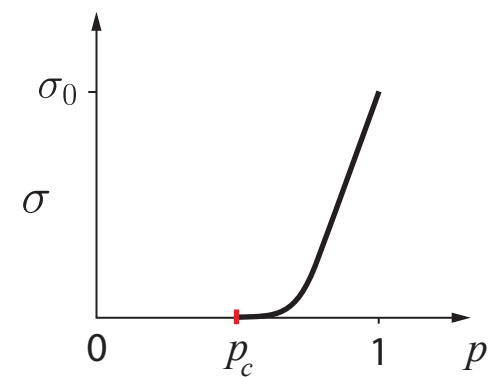


$$P_\infty(p) \sim (p - p_c)^\beta$$

$$p \rightarrow p_c^+$$

transport

effective conductivity
or fluid permeability



$$\sigma(p) \sim \sigma_0 (p - p_c)^t$$

$$p \rightarrow p_c^+$$

UNIVERSAL critical exponents for lattices -- depend only on dimension

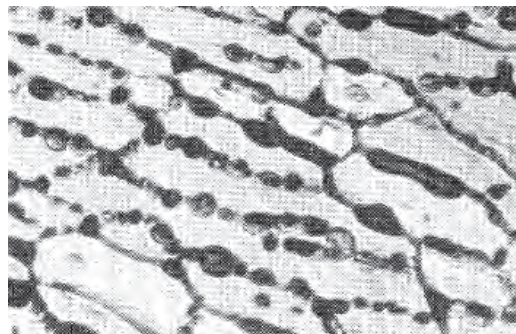
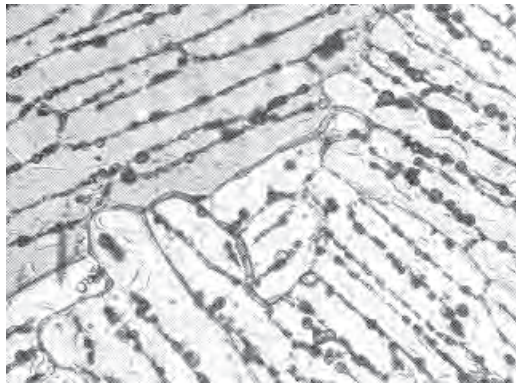
$1 \leq t \leq 2$ (for idealized model), Golden, *Phys. Rev. Lett.* 1990 ; *Comm. Math. Phys.* 1992

non-universal behavior in continuum

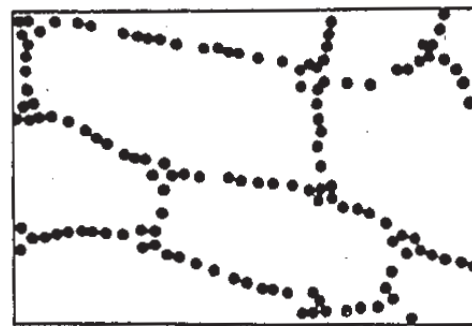
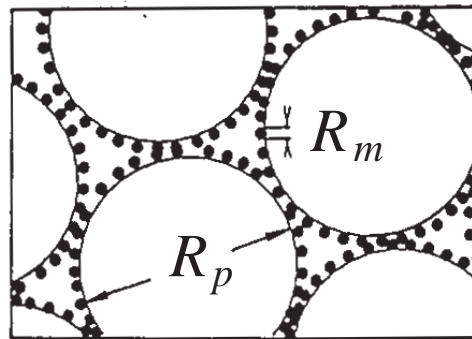
Continuum percolation model for **stealthy** materials applied to sea ice microstructure explains **Rule of Fives** and Antarctic data on **ice production** and **algal growth**

$$\phi_c \approx 5 \%$$

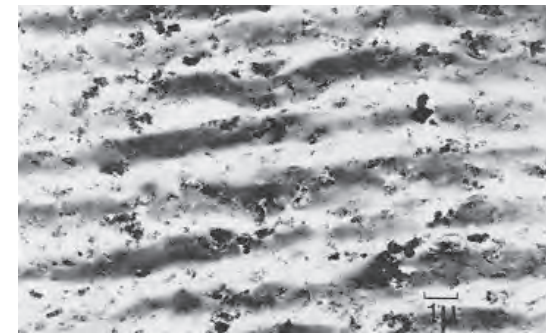
Golden, Ackley, Lytle, *Science*, 1998



sea ice



compressed
powder



radar absorbing
composite

sea ice is radar absorbing

**Geophysical
Research
Letters**

28 AUGUST 2007
Volume 34 Number 16
American Geophysical Union

***rigorous bounds
percolation theory
hierarchical model
network model***

field data

micro-scale
controls
macro-scale
processes

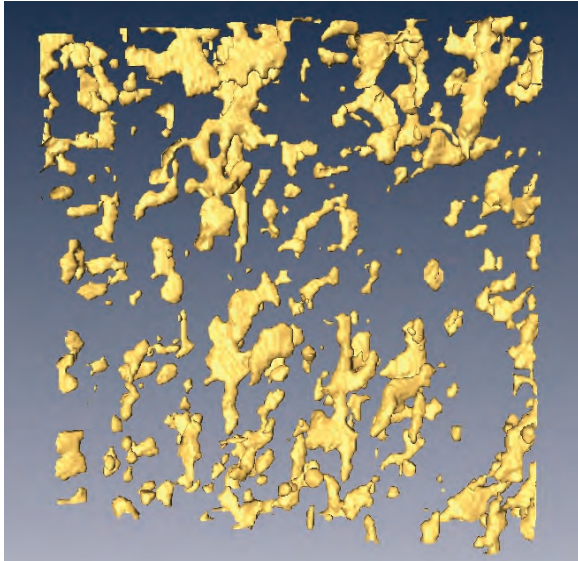
X-ray tomography for
brine inclusions

***unprecedented look
at thermal evolution
of brine phase and
its connectivity***

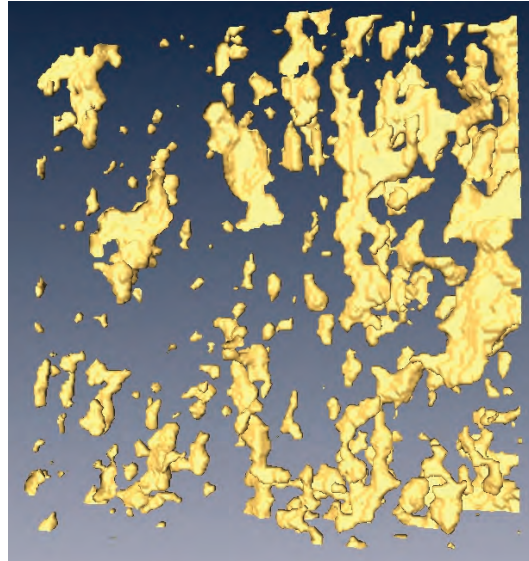
A unified approach to understanding permeability in sea ice • Solving the mystery of
booming sand dunes • Entering into the "greenhouse century": A case study from Switzerland

brine connectivity (over cm scale)

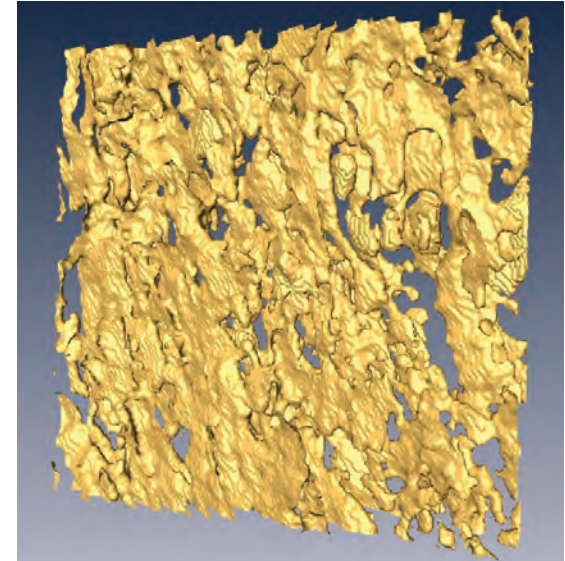
8 x 8 x 2 mm



-15 °C, $\phi = 0.033$



-6 °C, $\phi = 0.075$



-3 °C, $\phi = 0.143$

X-ray tomography confirms percolation threshold

3-D images
pores and throats



3-D graph
nodes and edges

analyze graph connectivity as function of temperature and sample size

- ***use finite size scaling techniques to confirm rule of fives***
- ***order parameter data from a natural material***

lattice and continuum percolation theories yield:

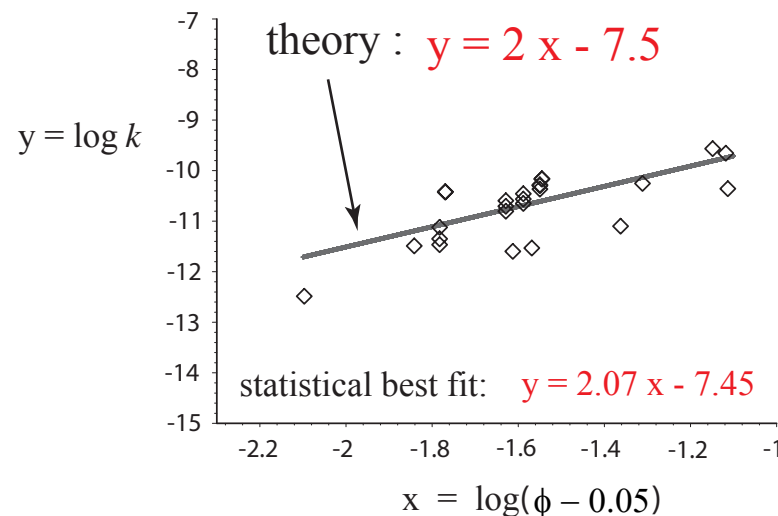
$$k(\phi) = k_0 (\phi - 0.05)^2$$

critical
exponent

$$k_0 = 3 \times 10^{-8} \text{ m}^2$$

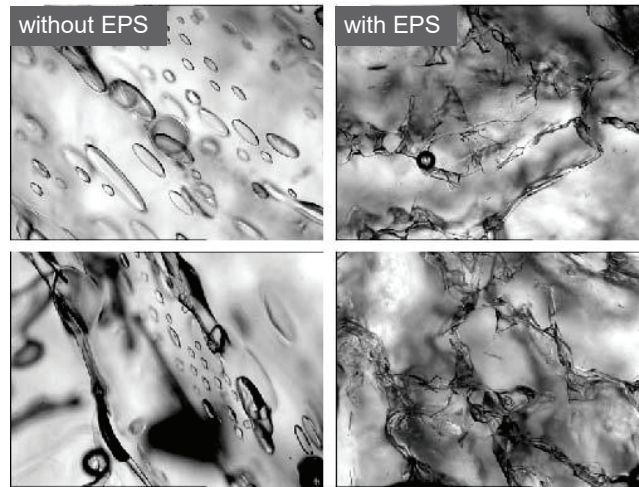
t

- exponent is **UNIVERSAL** lattice value $t \approx 2.0$
- **sedimentary rocks** like sandstones also exhibit universality
- **critical path analysis** -- developed for electronic hopping conduction -- yields scaling factor k_0

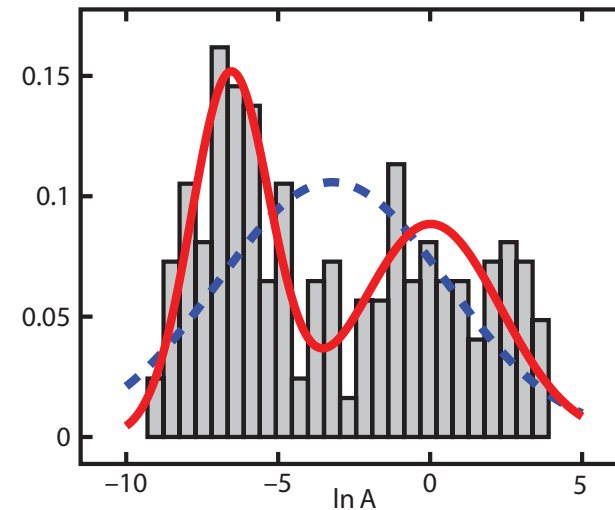


Sea ice algae secrete extracellular polymeric substances (EPS) affecting evolution of brine microstructure.

How does EPS affect fluid transport?



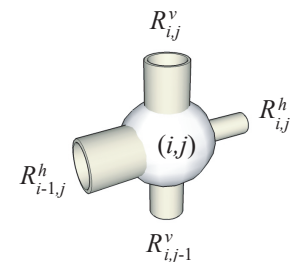
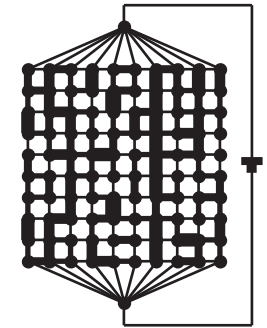
Krembs, Eicken, Deming, PNAS 2011



- **Bimodal** lognormal distribution for brine inclusions
- Develop random pipe network model with bimodal distribution; Use numerical methods that can handle larger variances in sizes.
- Results predict observed drop in fluid permeability k .
- Rigorous bound on k for bimodal distribution of pore sizes

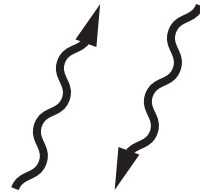
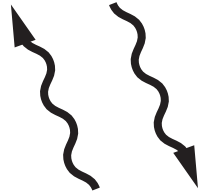
Steffen, Epshteyn, Zhu, Bowler, Deming, Golden 2017

How does the biology affect the physics?



Zhu, Jabini, Golden, Eicken, Morris
Ann. Glac. 2006

Remote sensing of sea ice



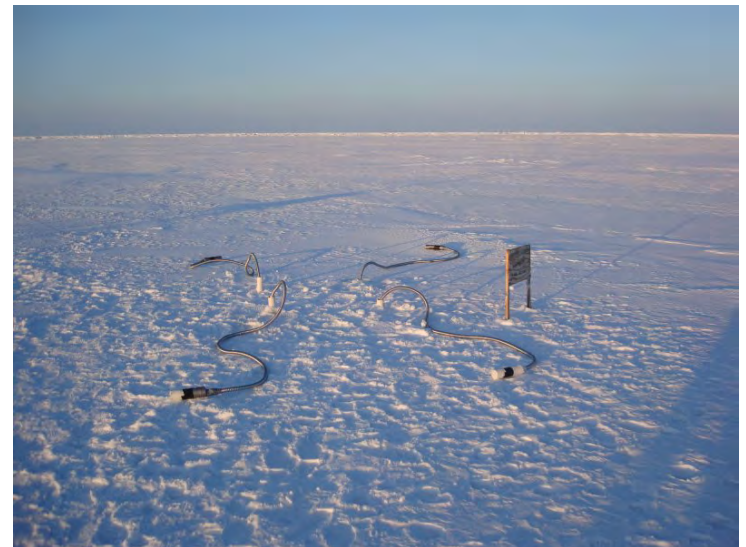
sea ice thickness
ice concentration

INVERSE PROBLEM

Recover sea ice
properties from
electromagnetic
(EM) data

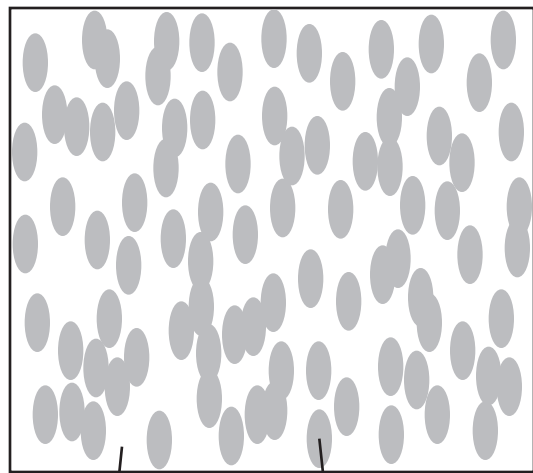
$$\epsilon^*$$

effective complex permittivity
(dielectric constant, conductivity)



brine volume fraction
brine inclusion connectivity

Effective complex permittivity of a two phase composite in the quasistatic (long wavelength) limit



ϵ_1

ϵ_2



ϵ^*

$$D = \epsilon E$$

$$\nabla \cdot D = 0$$

$$\nabla \times E = 0$$

$$\langle D \rangle = \epsilon^* \langle E \rangle$$

p_1, p_2 = volume fractions of
the components

$$\epsilon^* = \epsilon^* \left(\frac{\epsilon_1}{\epsilon_2}, \text{ composite geometry} \right)$$

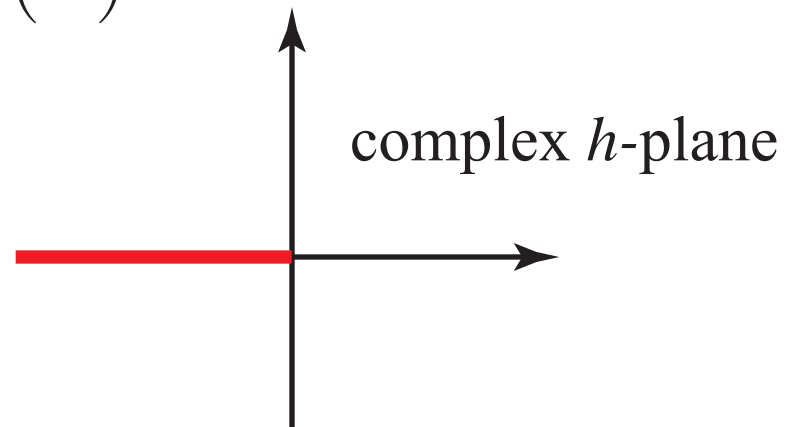
Analytic continuation method for bounding complex ϵ^*

Bergman (1978), Milton (1979), Golden and Papanicolaou (1983)

$$m(h) = \frac{\epsilon^*}{\epsilon_2} \left(\frac{\epsilon_1}{\epsilon_2} \right) \quad h = \frac{\epsilon_1}{\epsilon_2}$$

Exploit analytic properties of $m(h)$

- $m(h)$ analytic off negative real axis



- $m(h) : \text{UHP} \longrightarrow \text{UHP}$

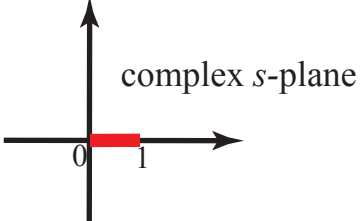
Theory of Effective Electromagnetic Behavior of Composites

analytic continuation method

Forward Homogenization Bergman (1978), Milton (1979), Golden and Papanicolaou (1983)
Theory of Composites, Milton (2002)

composite geometry
(spectral measure μ) \longrightarrow ϵ^*

integral representations, rigorous bounds, approximations, etc.

$$F(s) = 1 - \frac{\epsilon^*}{\epsilon_2} = \int_0^1 \frac{d\mu(z)}{s - z} \quad s = \frac{1}{1 - \epsilon_1 / \epsilon_2}$$


The diagram shows a complex plane with a horizontal real axis and a vertical imaginary axis. A red line segment on the real axis represents a branch cut, extending from the origin (labeled 0) to the point 1. The text 'complex s-plane' is written in the upper right quadrant.

Inverse Homogenization Cherkaev and Golden (1998), Day and Thorpe (1999), Cherkaev (2001)
McPhedran, McKenzie, Milton (1982), *Theory of Composites*, Milton (2002)

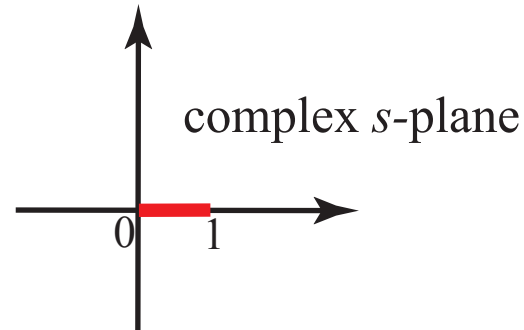
ϵ^* \longrightarrow ***composite geometry***
(spectral measure μ)

recover brine volume fraction, connectivity, etc.

Stieltjes integral representation

separation of geometry from parameters

$$s = \frac{1}{1 - \epsilon_1 / \epsilon_2}$$



$$F(s) = 1 - \frac{\epsilon^*}{\epsilon_2} = \int_0^1 \frac{d\mu(z)}{s - z}$$

- μ /
- spectral measure of self adjoint operator $\Gamma\chi$
 - mass = p_1
 - higher moments depend on n -point correlations

$$\Gamma = \nabla(-\Delta)^{-1}\nabla.$$

χ = characteristic function of the brine phase

$$E = (s + \Gamma\chi)^{-1}e_k$$

using the Stieltjes integral representation to obtain bounds

“linear programming” Golden and Papanicolaou, *CMP* 1983

M_1 = the set of positive Borel measures on $[0,1]$, compact, convex

$F_s(\mu) : M_1 \longrightarrow \mathbb{C}$ linear functional

extremal values (bounds) are images of extreme points of M_1

Dirac point measures $\frac{\mu_0}{s - z^*}$

higher order bounds -- iterated fractional linear transformations

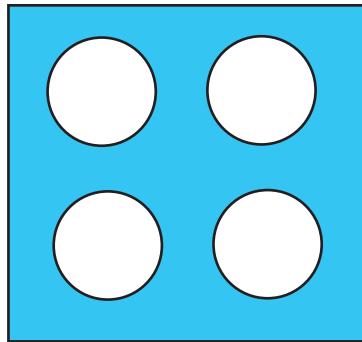
$$F_1(s) = \frac{1}{\mu_0} - \frac{1}{sF(s)}$$



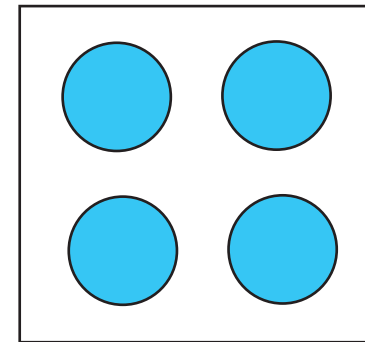
Baker 1969
Milton 1981
Bergman 1982
Felderhof 1984
Golden 1986

Keller Interchange Theorem

J. B. Keller, *J. Math. Phys.* 1964



two dimensional
two phase
composites
 $\sigma_1 \quad \sigma_2$



$$\sigma_{xx}^*(\sigma_1, \sigma_2) \sigma_{yy}^*(\sigma_2, \sigma_1) = \sigma_1 \sigma_2$$

isotropic media

$$\sigma^*(\sigma_1, \sigma_2) \sigma^*(\sigma_2, \sigma_1) = \sigma_1 \sigma_2$$

$d = 3$ inequality
Shulgasser *JMP* 1976

$d = 2$ square bond lattice $1, h$
conductivity of random checkerboard

$$\sigma^*(p_c = 1/2) = \sqrt{h}, \quad h \longrightarrow 0$$

**effective transport in two dimensional
quasiperiodic media**

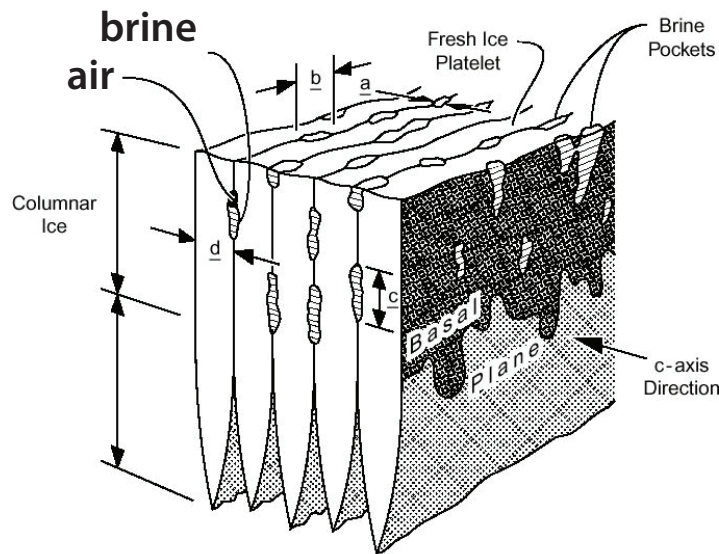
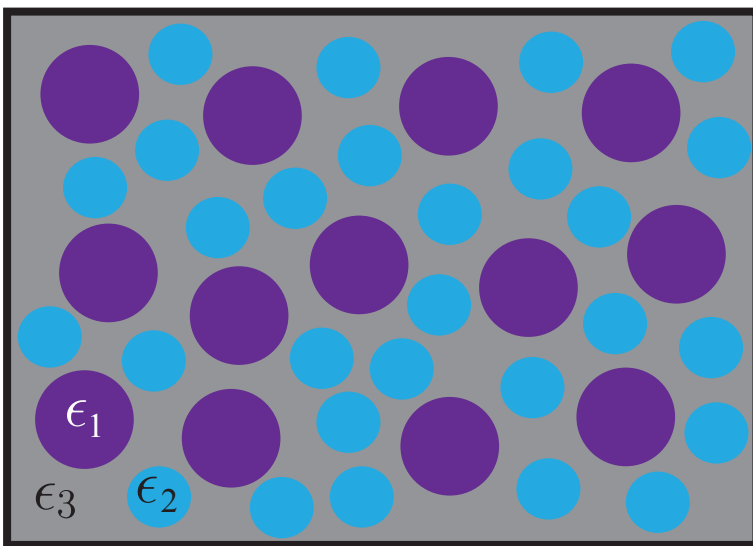
Golden, Goldestein, Lebowitz, *J. Stat. Phys.* 1990

Multiphase Media

polydisc representation formula for Herglotz function in several complex variables; bounds on effective parameters

Golden and Papanicolaou, *J. Stat. Phys.* 1985

Golden, *J. Mech. Phys. Solids* 1986



$$m(h_1, h_2) = \epsilon^*/\epsilon_3 \quad h_i = \epsilon_i/\epsilon_3 \quad i = 1, 2$$

$$F(s_1, s_2) = 1 - m(h_1, h_2)$$

$$s_i = 1/(1 - h_i) \quad \zeta_j = \frac{s_j - i}{s_j + i}$$

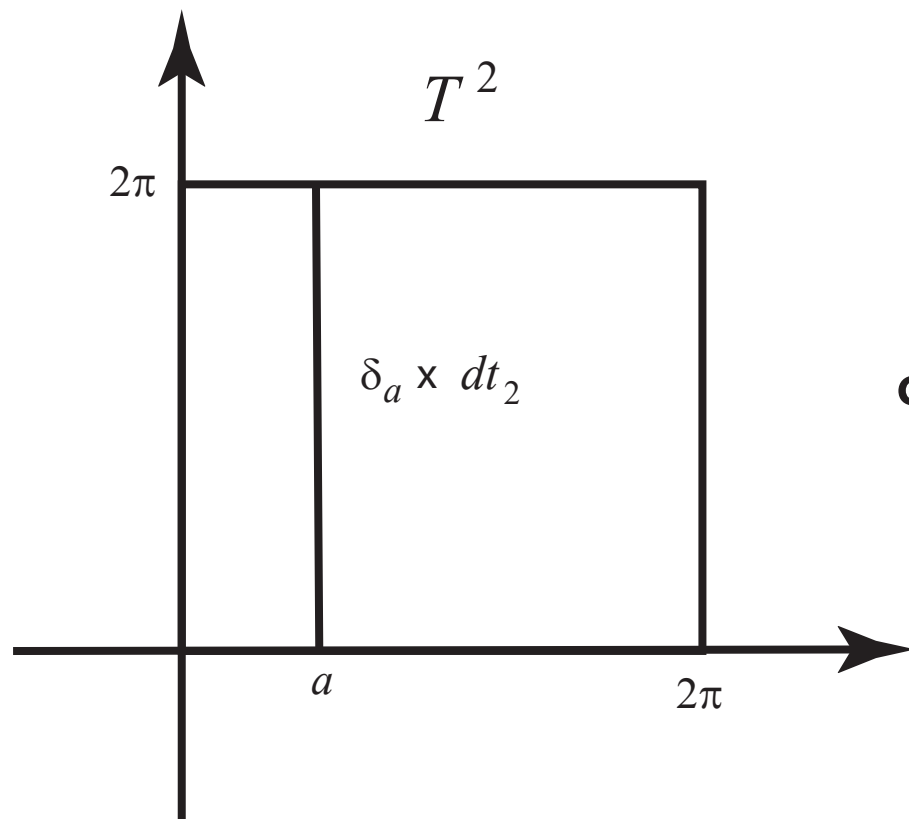
$$f(\zeta_1, \zeta_2) = iF(s_1, s_2) \quad f(\zeta_1, \zeta_2) : D^2 \rightarrow \{Re f > 0\}$$

$$f(\zeta_1, \zeta_2) = iImf(0, 0) + \frac{1}{2} \int_0^{2\pi} \int_0^{2\pi} (H_1 H_2 + H_1 + H_2 - 1) \mu(dt_1, dt_2)$$

$$H_1 = (e^{it_1} + \zeta_1)/(e^{it_1} - \zeta_1) \quad H_2 = (e^{it_2} + \zeta_2)/(e^{it_2} - \zeta_2)$$

μ is a positive Borel measure on the torus T^2

satisfying a Fourier condition (excludes point measures)



conjectured extremals yield bounds

set of extremal measures = ??

Herglotz-Nevanlinna functions and their applications
8-12 May 2017, Institut Mittag-Leffler, Stockholm

field equation recursion method

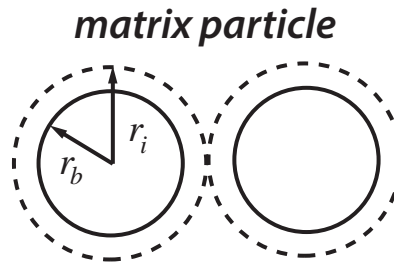
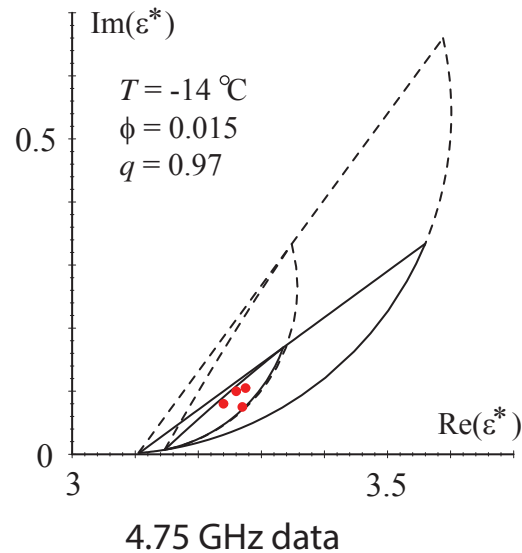
Milton, *Comm. Math. Phys. (I and II)* 1987

effective elasticity tensor

Ou, *Complex Vars. Elliptic. Eqs.* 2011

forward and inverse bounds on the complex permittivity of sea ice

forward bounds



$$q = r_b / r_i$$

$$0 < q < 1$$

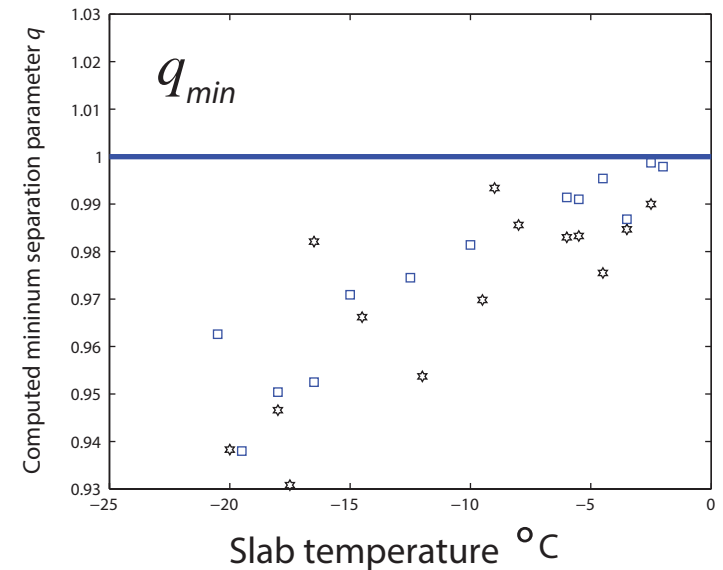
Golden 1995, 1997

Bruno 1991

inverse bounds and recovery of brine porosity

**Gully, Backstrom, Eicken, Golden
Physica B, 2007**

inverse bounds



inversion for brine inclusion separations in sea ice from measurements of effective complex permittivity ϵ^*

rigorous inverse bound on spectral gap

construct algebraic curves which bound admissible region in (p, q) -space

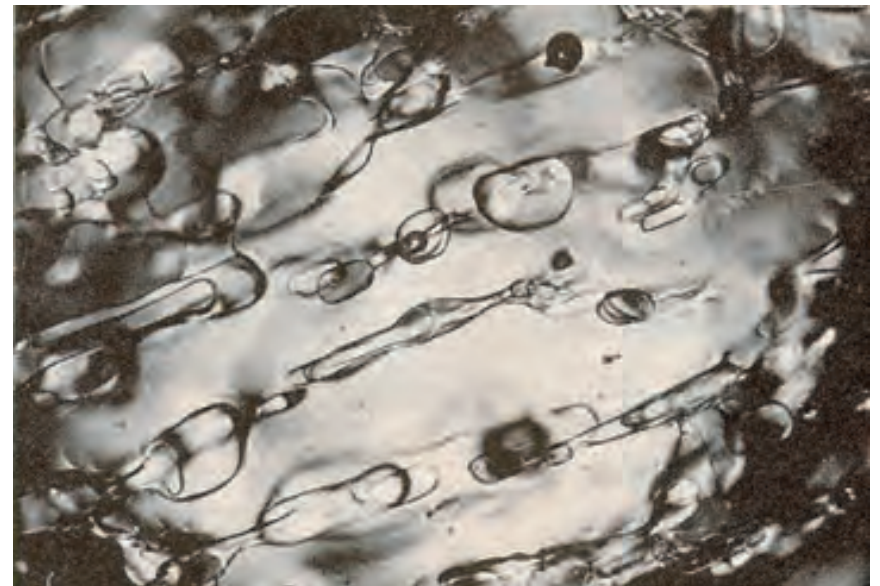
**Orum, Cherkaev, Golden
Proc. Roy. Soc. A, 2012**

the math doesn't care if it's sea ice or bone!

HUMAN BONE



SEA ICE



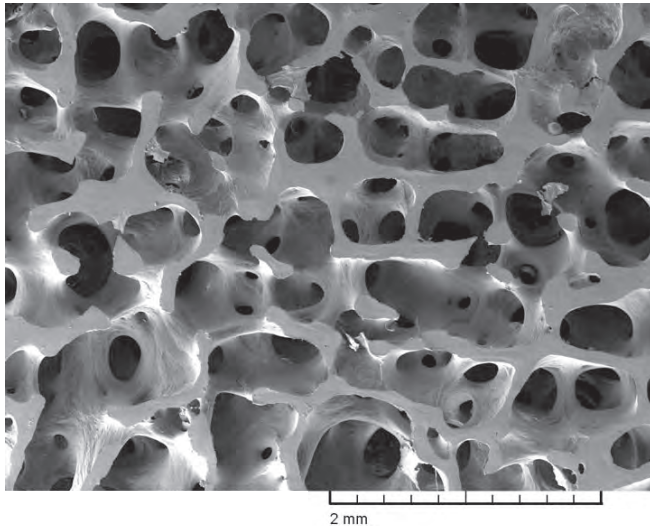
***apply spectral measure analysis of brine connectivity and
spectral inversion to electromagnetic monitoring osteoporosis***

Golden, Murphy, Cherkaev, J. Biomechanics 2011

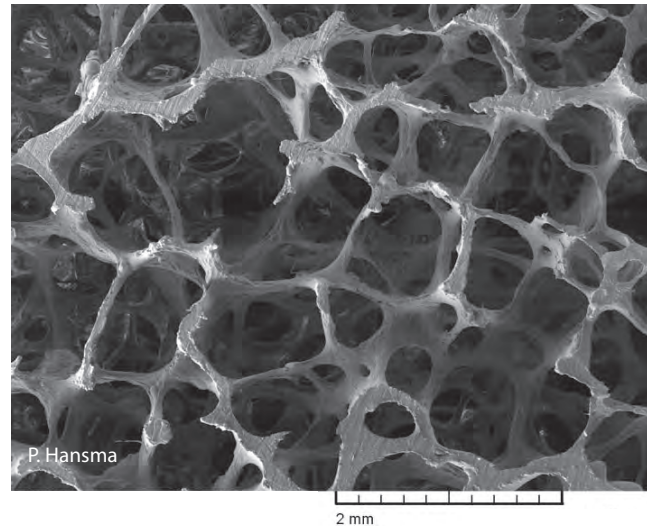
spectral characterization of porous microstructures in bone

Golden, Murphy, Cherkaev, J. Biomechanics 2011

(a) young healthy trabecular bone



(b) old osteoporotic trabecular bone



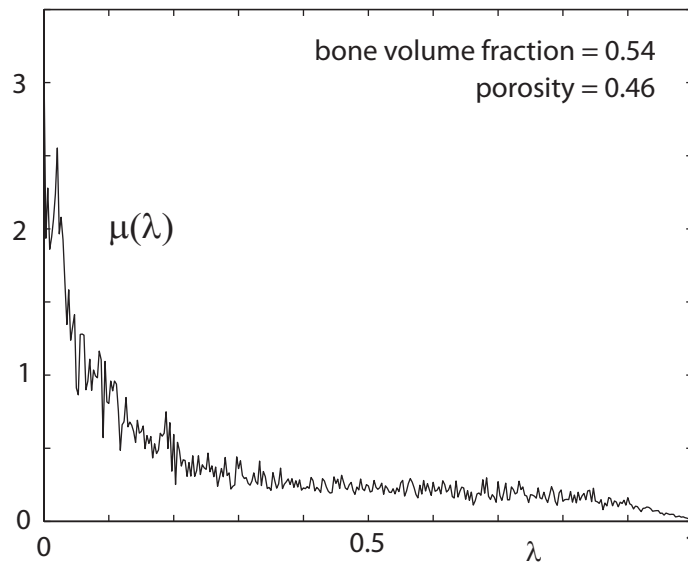
+

reconstruction of spectral
measures from complex
permittivity data

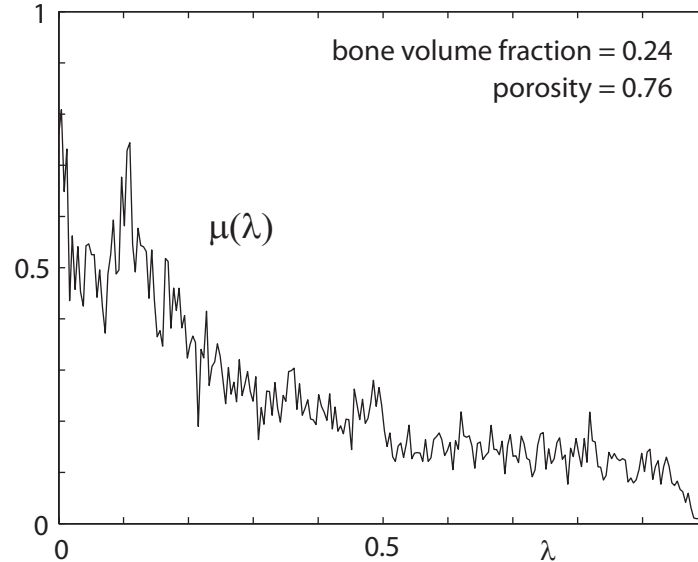
*using regularized
inversion scheme*



(c) spectral measure - young



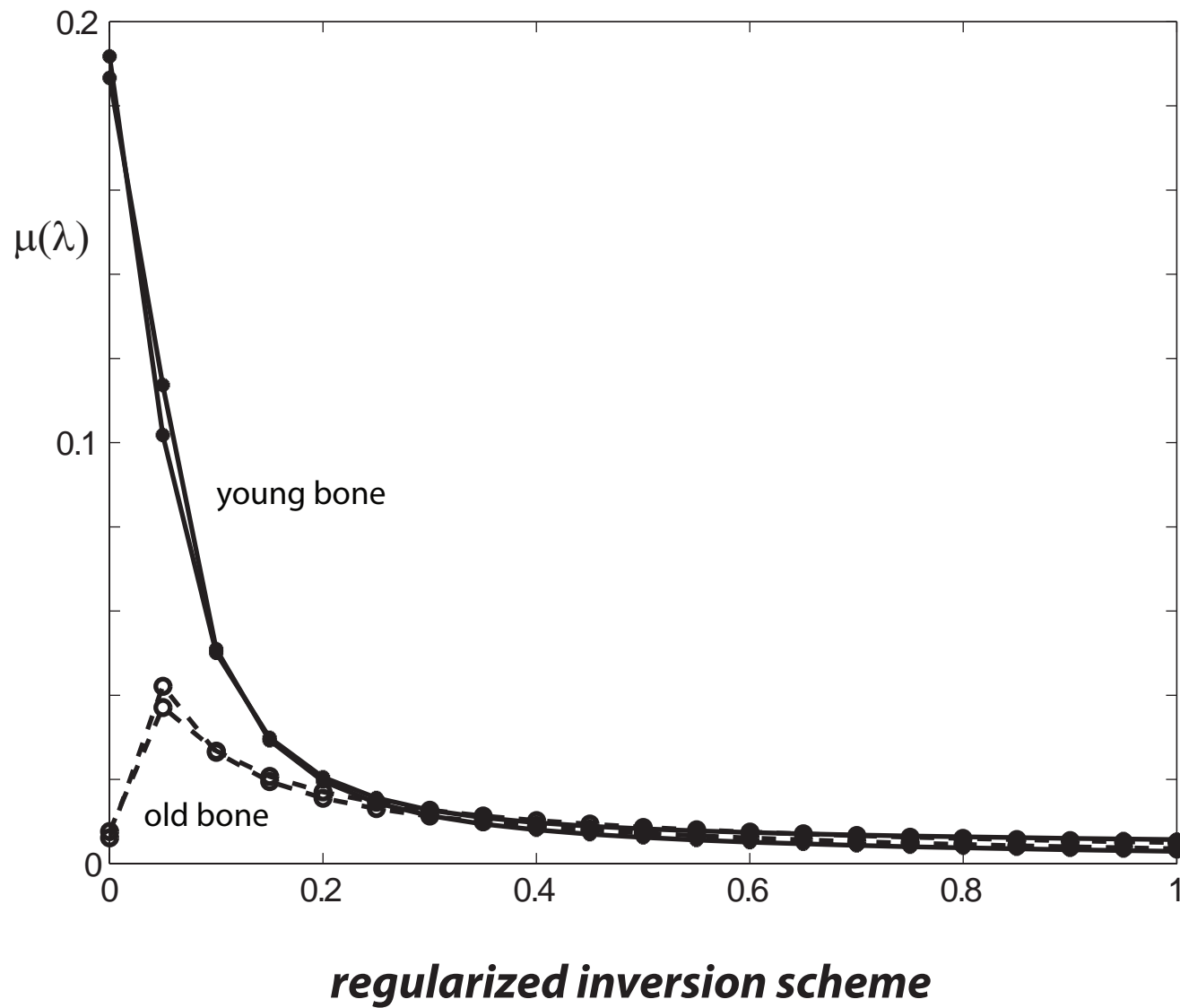
(d) spectral measure - old



***EM monitoring
of osteoporosis***

***loss of bone
connectivity***

reconstruction of spectral measures from simulated complex permittivity data



direct calculation of spectral measure

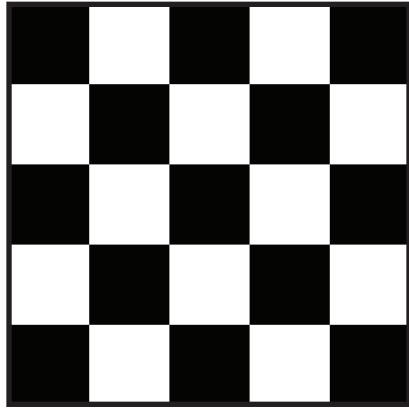
1. Discretization of composite microstructure gives lattice of 1's and 0's (random resistor network).
2. The fundamental operator $\chi\Gamma\chi$ becomes a random matrix depending only on the composite geometry.
3. Compute the eigenvalues λ_i and eigenvectors of $\chi\Gamma\chi$ with inner product weights α_i

$$\mu(\lambda) = \sum_i \alpha_i \delta(\lambda - \lambda_i)$$



Dirac point measure (Dirac delta)

Continuum composite

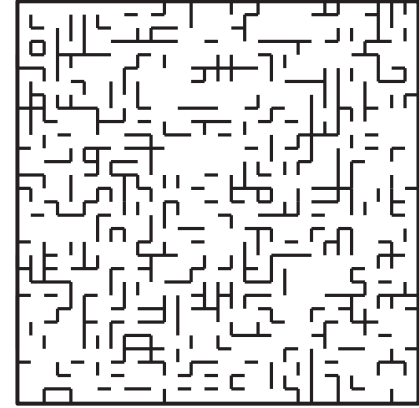


Spectral measures of

$$\chi_1 \Gamma \chi_1$$

Murphy, Hohenegger, Cherkaev, Golden
Comm. Math. Sci. 2015

Discrete composite



Integro-differential projection operator

$$\Gamma = \vec{\nabla}(\Delta^{-1})\vec{\nabla}.$$

Point-wise indicator function

$$\chi_1$$

Resolvent representation of electric field

$$\chi_1 \vec{E} = sE_0(sI - \chi_1 \Gamma \chi_1)^{-1} \chi_1 \vec{e}_k$$

Integral representation

$$F(s) = \int_0^1 \frac{d\mu(\lambda)}{s - \lambda}$$

Projection matrix

$$\Gamma = \nabla(\nabla^T \nabla)^{-1} \nabla^T$$

Diagonal projection matrix

$$\chi_1$$

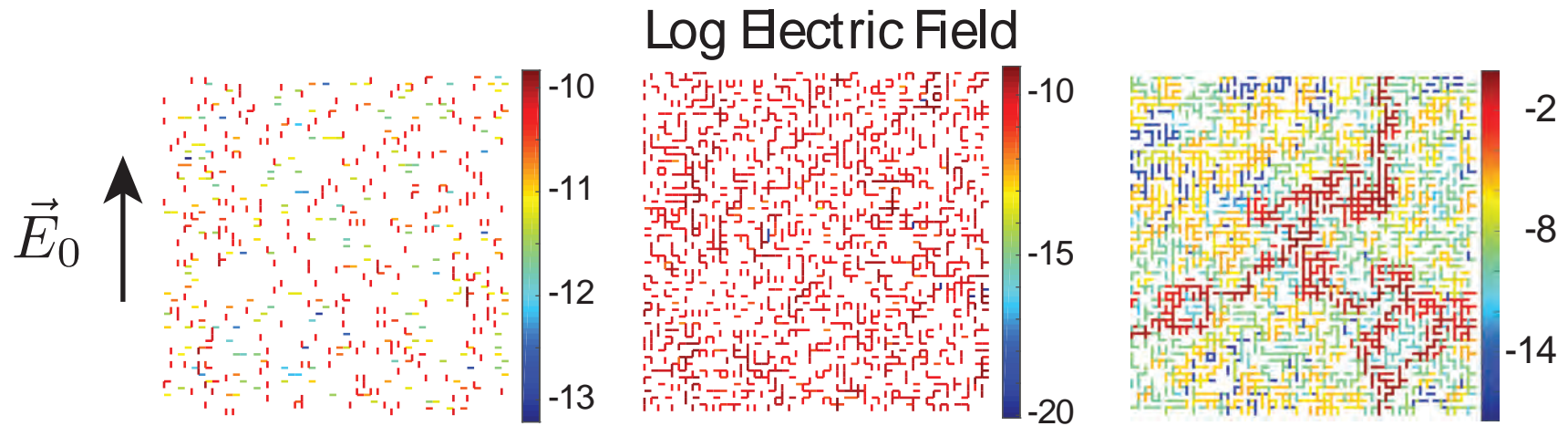
Series representation of electric field

$$\chi_1 \vec{E} = sE_0 \sum_j \frac{\vec{v}_j \cdot \chi_1 \vec{e}_k}{s - \lambda_j} \vec{v}_j$$

Series representation

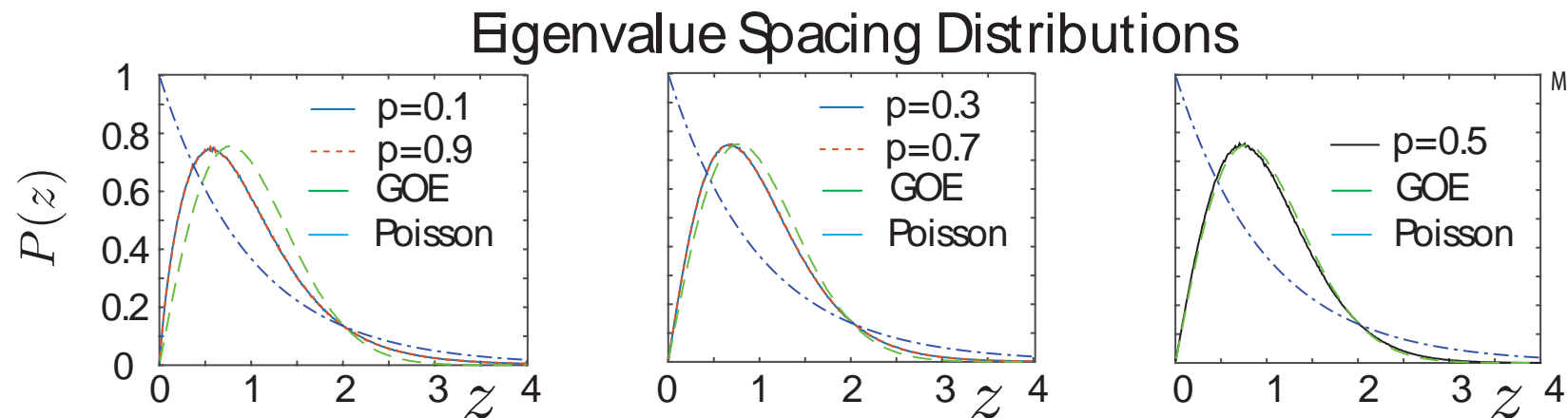
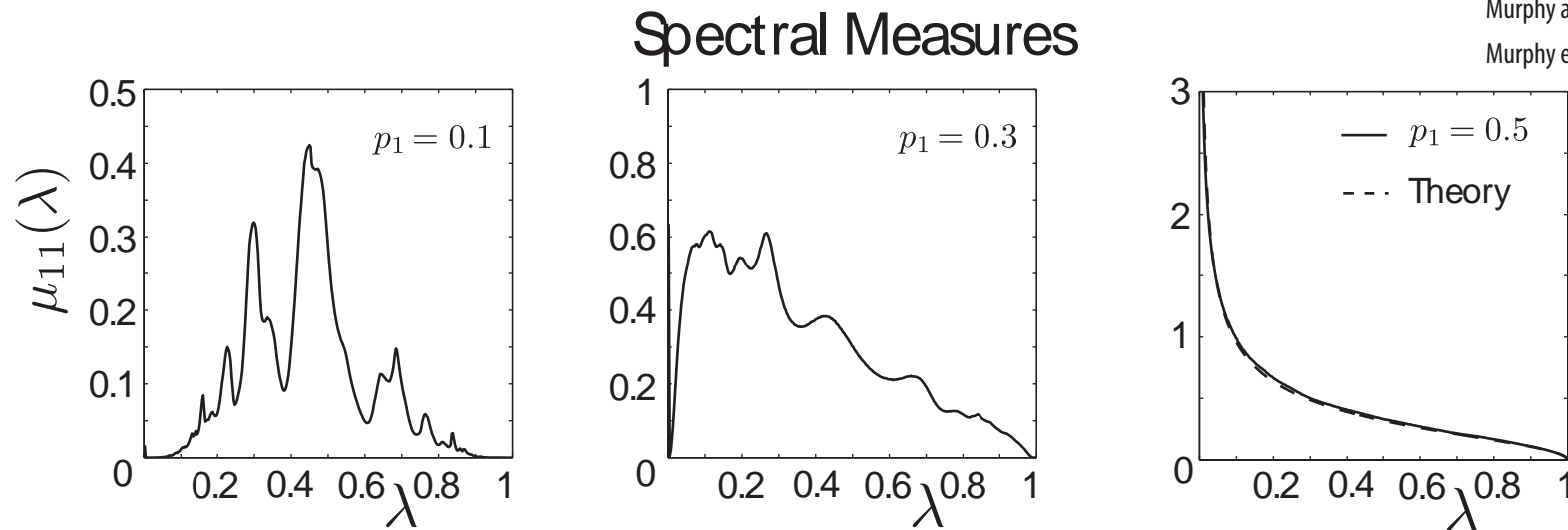
$$F(s) = \sum_j \frac{(\vec{v}_j \cdot \chi_1 \vec{e}_k)^2}{s - \lambda_j}$$

Spectral statistics for 2D random resistor network



Murphy and Golden, J. Math. Phys., 2012

Murphy et al. Comm. Math. Sci., 2015



Murphy, Cherkhev, Golden, 2016

Eigenvalue Statistics of Random Matrix Theory

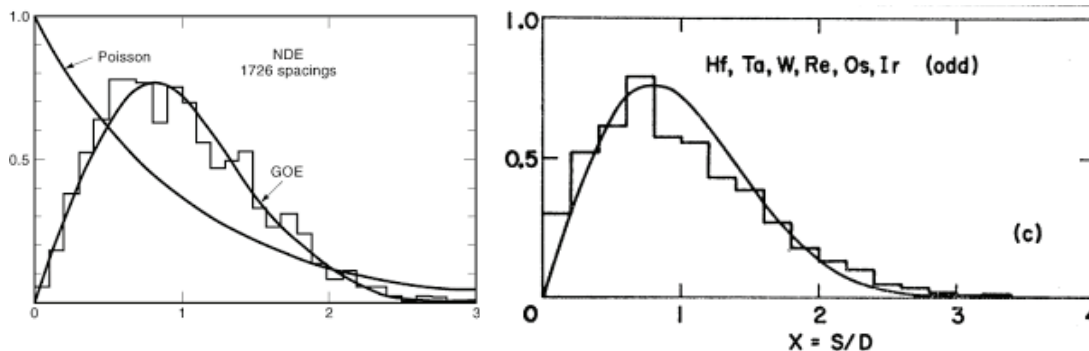
Wigner (1951) and Dyson (1953) first used random matrix theory (RMT) to describe quantized energy levels of heavy atomic nuclei.

$[N]_{ij} \sim N(0,1), \quad A = (N + N^T)/2 \quad \text{Gaussian orthogonal ensemble (GOE)}$

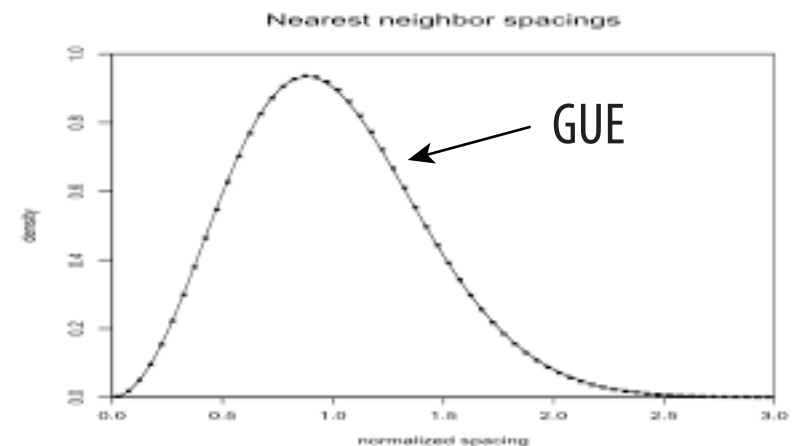
$[N]_{ij} \sim N(0,1) + iN(0,1), \quad A = (N + N^\dagger)/2 \quad \text{Gaussian unitary ensemble (GUE)}$

Short range and long range correlations of eigenvalues are measured by various eigenvalue statistics

Spacing distributions of energy levels for heavy atomic nuclei



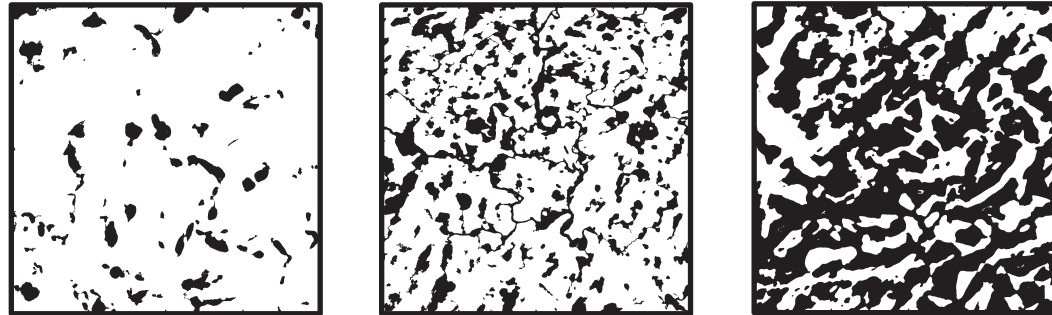
Spacing distributions of the first billion zeros of the Riemann zeta function



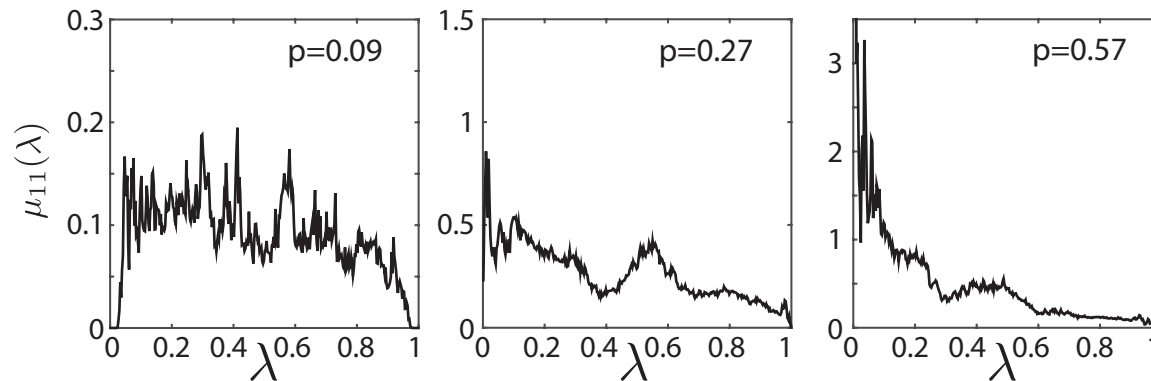
RMT used to characterize **disorder-driven transitions** in mesoscopic conductors, neural networks, random graph theory, etc.

Phase transitions \sim transitions in **universal eigenvalue statistics**.

Spectral computations for Arctic melt ponds

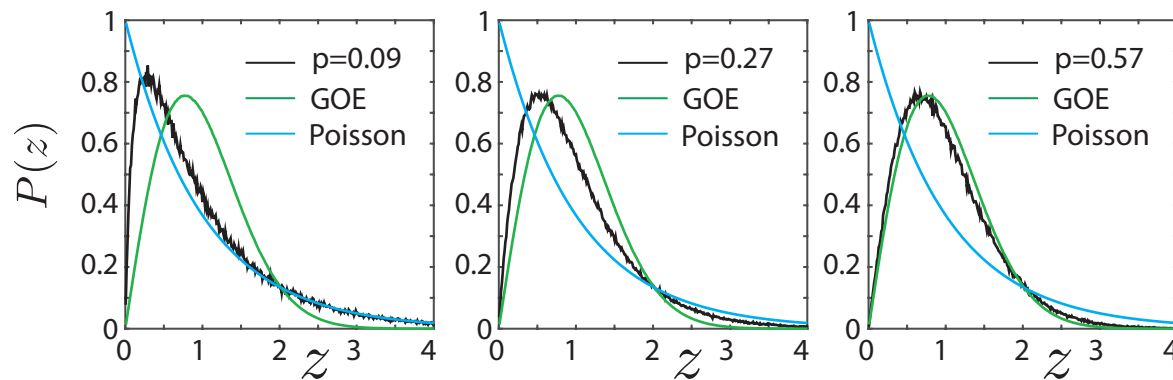


spectral
measures



Ben Murphy
Elena Cherkaev
Ken Golden
2017

eigenvalue
spacing
distributions



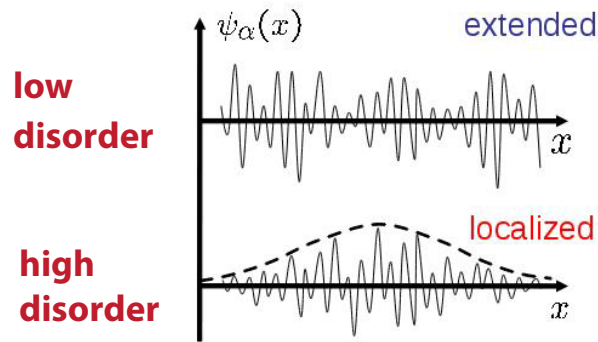
uncorrelated



level repulsion

TRANSITION

*eigenvalue statistics
for transport tend
toward the
UNIVERSAL
Wigner-Dyson
distribution
as the “conducting”
phase percolates*



metal / insulator transition

localization

Anderson 1958
Mott 1949
Shklovshii et al 1993
Evangelou 1992

Anderson transition in wave physics:
 quantum, optics, acoustics, water waves, ...

we find a surprising analog

Anderson transition for classical transport in composites

Murphy, Cherkaev, Golden Phys. Rev. Lett. 2017

**PERCOLATION
TRANSITION**



**transition to universal
eigenvalue statistics (GOE)
extended states, mobility edges**

-- but without wave interference or scattering effects ! --

eigenvector localization and mobility edges

Inverse Participation Ratio:
$$I(\vec{v}_n) = \sum_{i=1}^N |(\vec{v}_n)_i|^4$$

Completely Localized:
$$I(\vec{e}_n) = 1$$

Completely Extended:
$$I\left(\frac{1}{\sqrt{N}} \vec{1}\right) = \frac{1}{N}$$

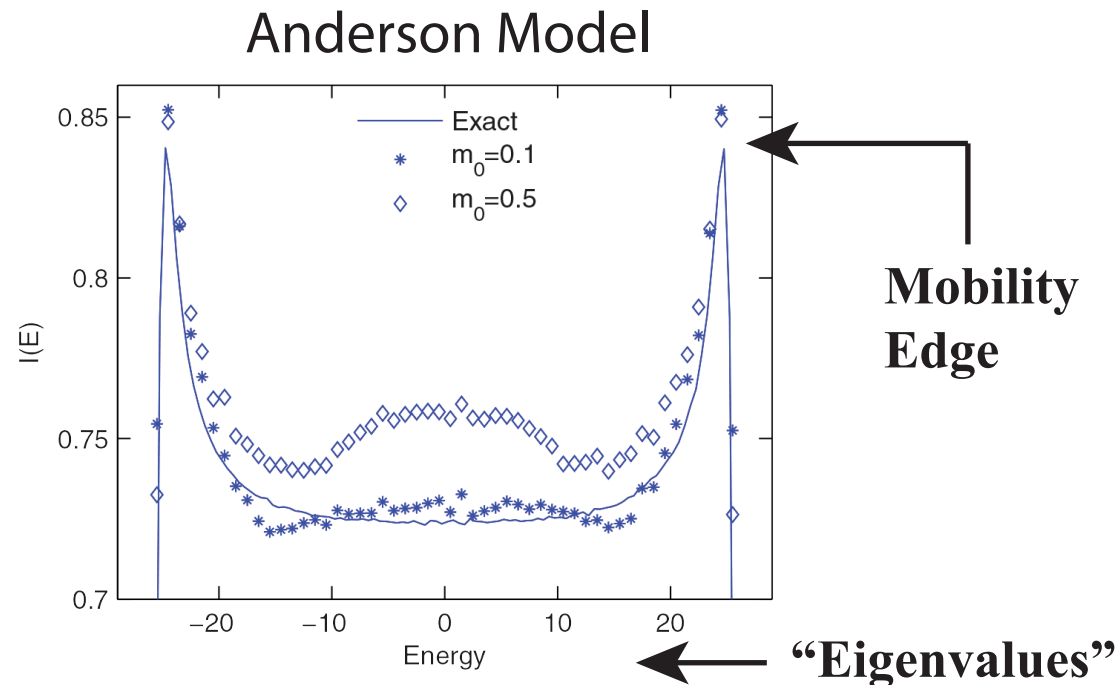
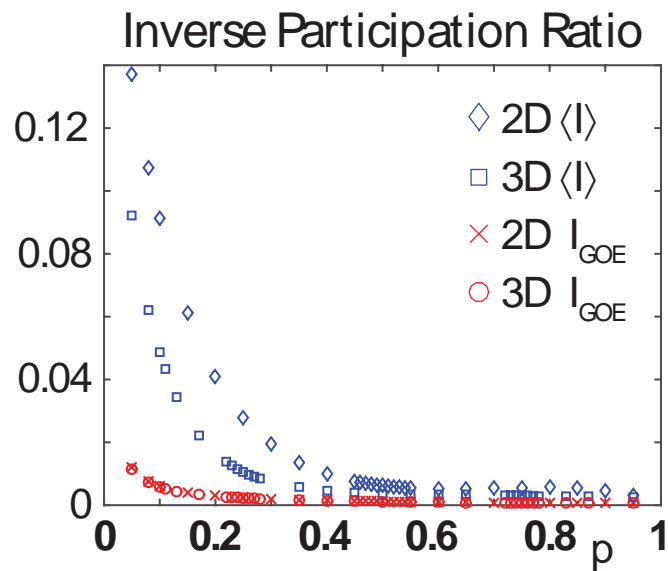
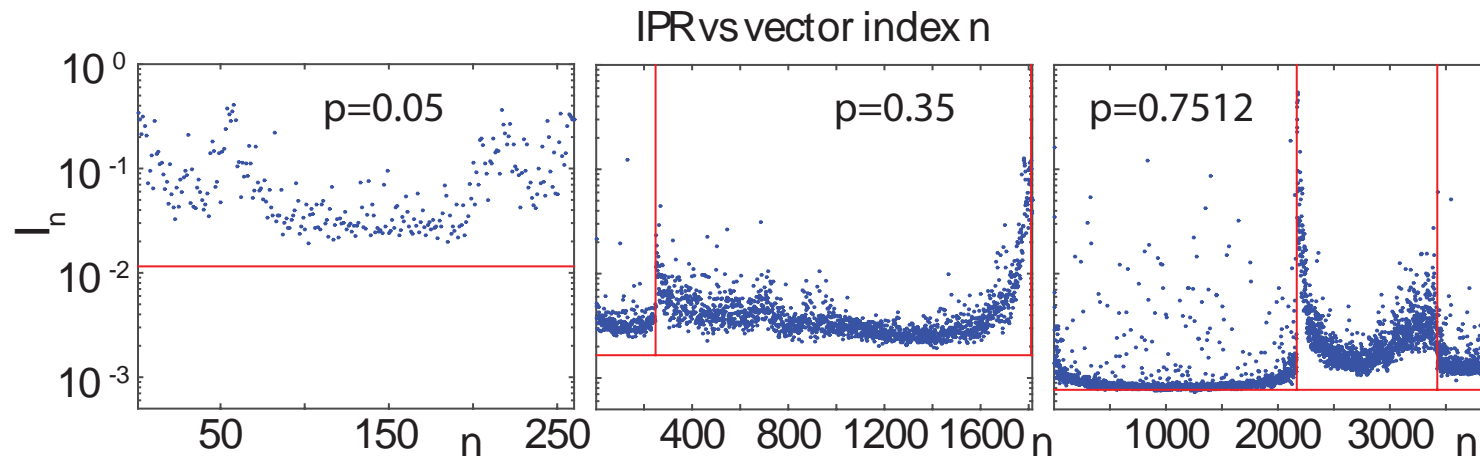


FIG. 4. (Color online) IPR for Anderson model in two dimensions with $x = 6.25$ ($w = 50$) from exact diagonalization (solid line) and from LDRG with different values of the cutoff m_0 . LDRG data are averaged over 100 runs of systems with 100×100 sites.

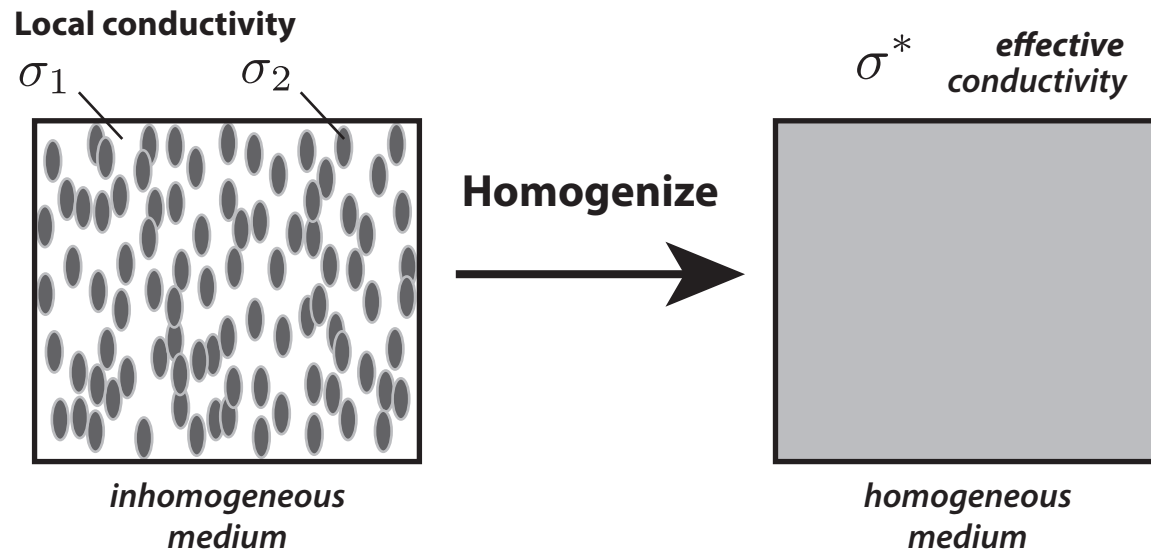
Localization properties of eigenvectors in random resistor networks



$$I_n = \sum_i (\vec{v}_n)_i^4$$

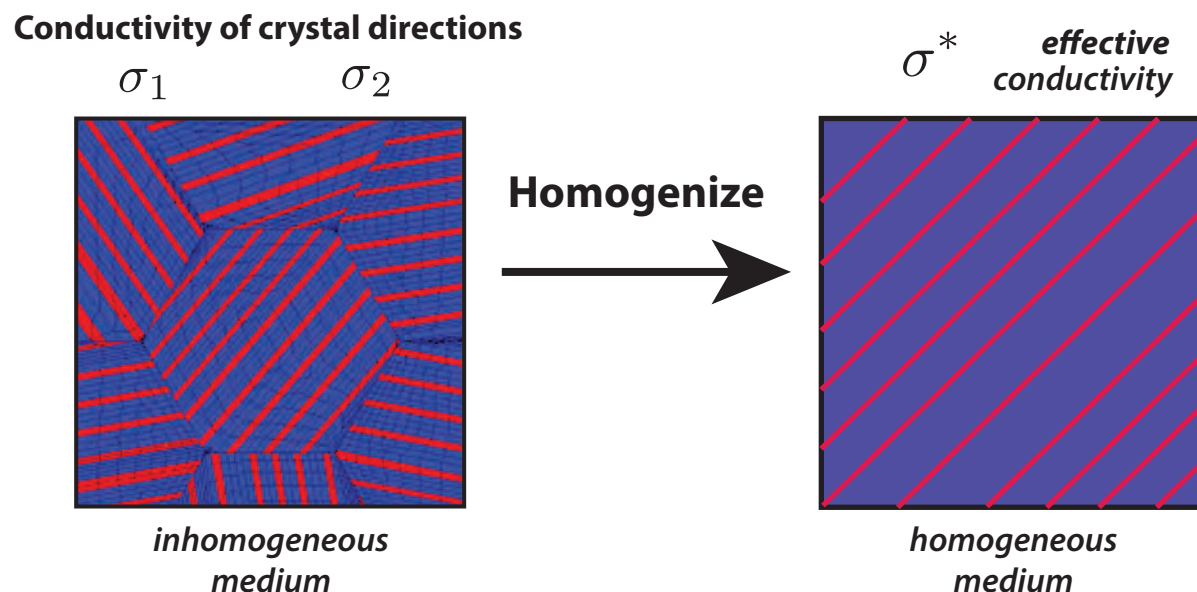
Homogenization for composite materials

**Two-component
composites**



Find the homogeneous medium which behaves macroscopically the same as the inhomogeneous medium

**Polycrystalline
media**



Bounds on the complex permittivity of polycrystalline materials by analytic continuation

Adam Gully, Joyce Lin,
Elena Cherkaev, Ken Golden

- **Stieltjes integral representation for effective complex permittivity**
Milton (1981, 2002), Barabash and Stroud (1999), ...
- **Forward and inverse bounds**
- **Applied to sea ice using two-scale homogenization**
- **Inverse bounds give method for distinguishing ice types using remote sensing techniques**



PROCEEDINGS A

350 YEARS
OF SCIENTIFIC
PUBLISHING

An invited review
commemorating 350 years
of scientific publishing at the
Royal Society

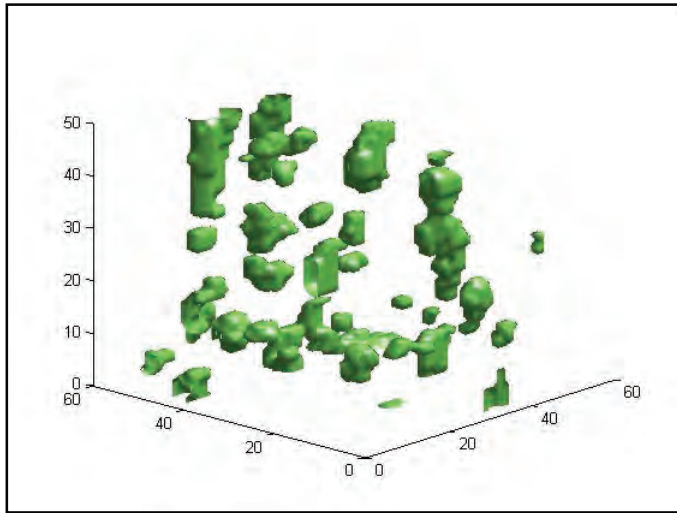
A method to distinguish
between different types
of sea ice using remote
sensing techniques

A computer model to
determine how a human
should walk so as to expend
the least energy

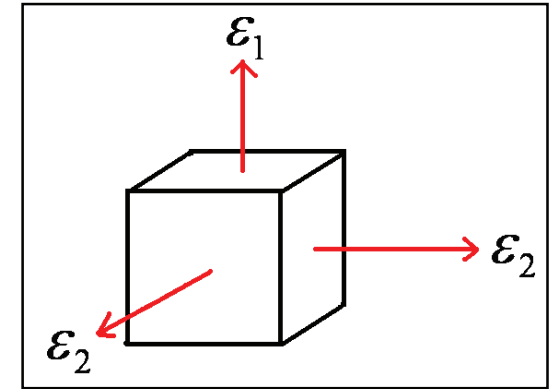


THE
ROYAL
SOCIETY
PUBLISHING

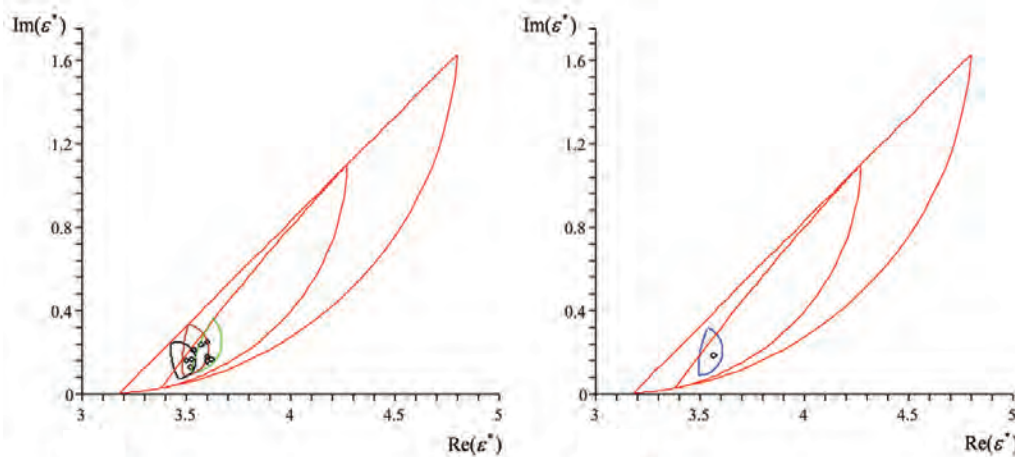
two scale homogenization for polycrystalline sea ice



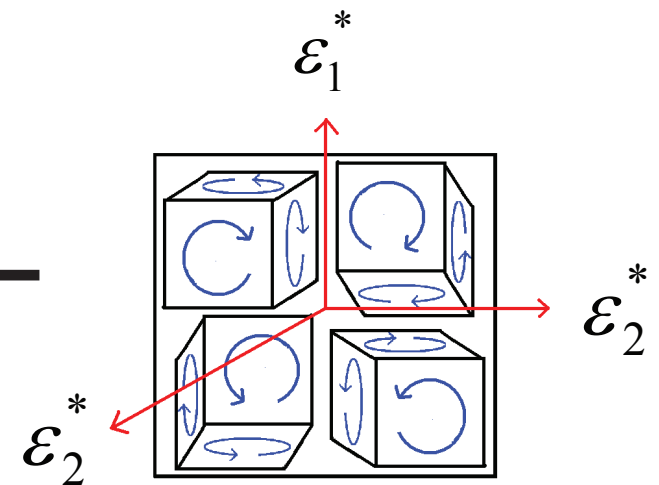
numerical homogenization
for single crystal



analytic continuation
for polycrystals



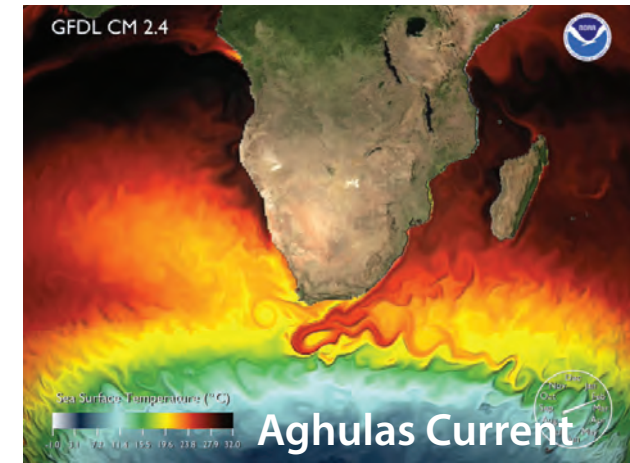
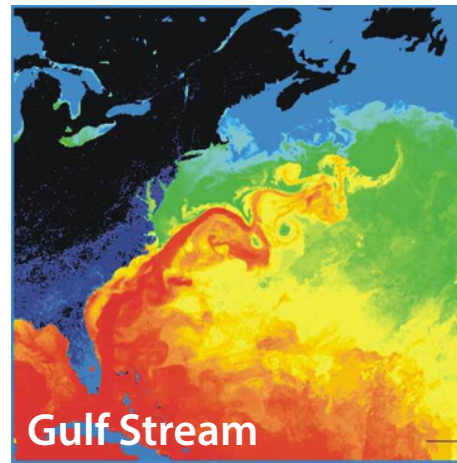
bounds



advection enhanced diffusion

effective diffusivity

tracers, buoys diffusing in ocean eddies
diffusion of pollutants in atmosphere
salt and heat transport in ocean
heat transport in sea ice with convection



advection diffusion equation with a velocity field \vec{u}

$$\frac{\partial T}{\partial t} + \vec{u} \cdot \vec{\nabla} T = \kappa_0 \Delta T$$

$$\vec{\nabla} \cdot \vec{u} = 0$$

homogenize

$$\frac{\partial \bar{T}}{\partial t} = \kappa^* \Delta \bar{T}$$

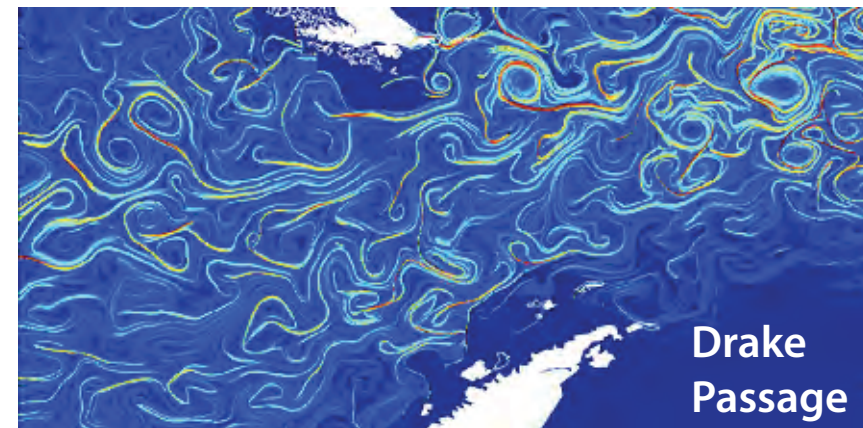
κ^* effective diffusivity

Stieltjes integral for κ^* with spectral measure

Avellaneda and Majda, PRL 89, CMP 91

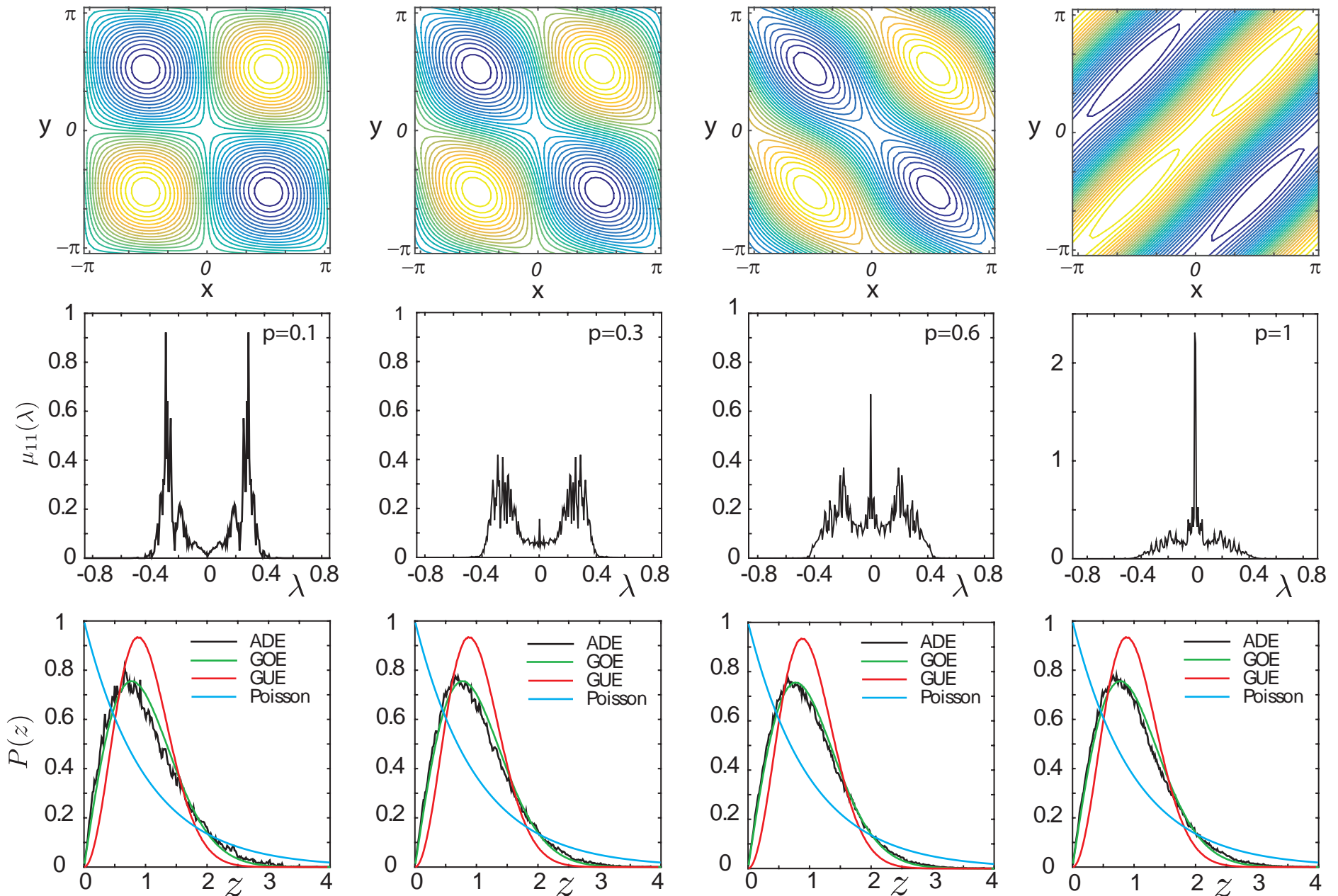
Murphy, Cherkaev, Xin, Zhu, Golden, *Ann. Math. Sci. Appl.* 2017

Murphy, Cherkaev, Zhu, Xin, Golden, 2017

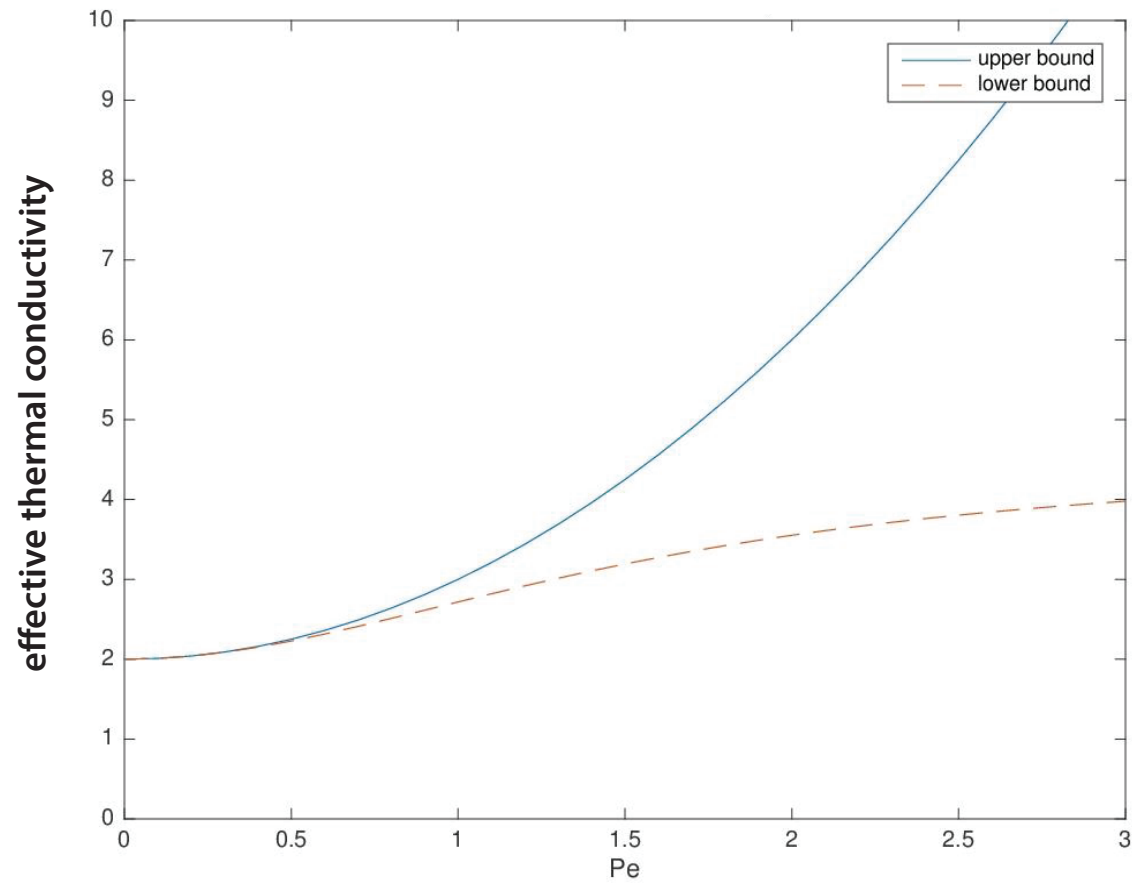


Spectral measures and eigenvalue spacings for cat's eye flow

$$H(x,y) = \sin(x) \sin(y) + A \cos(x) \cos(y), \quad A \sim U(-p,p)$$



bounds on the effective thermal conductivity of sea ice with convection (BC flow model)

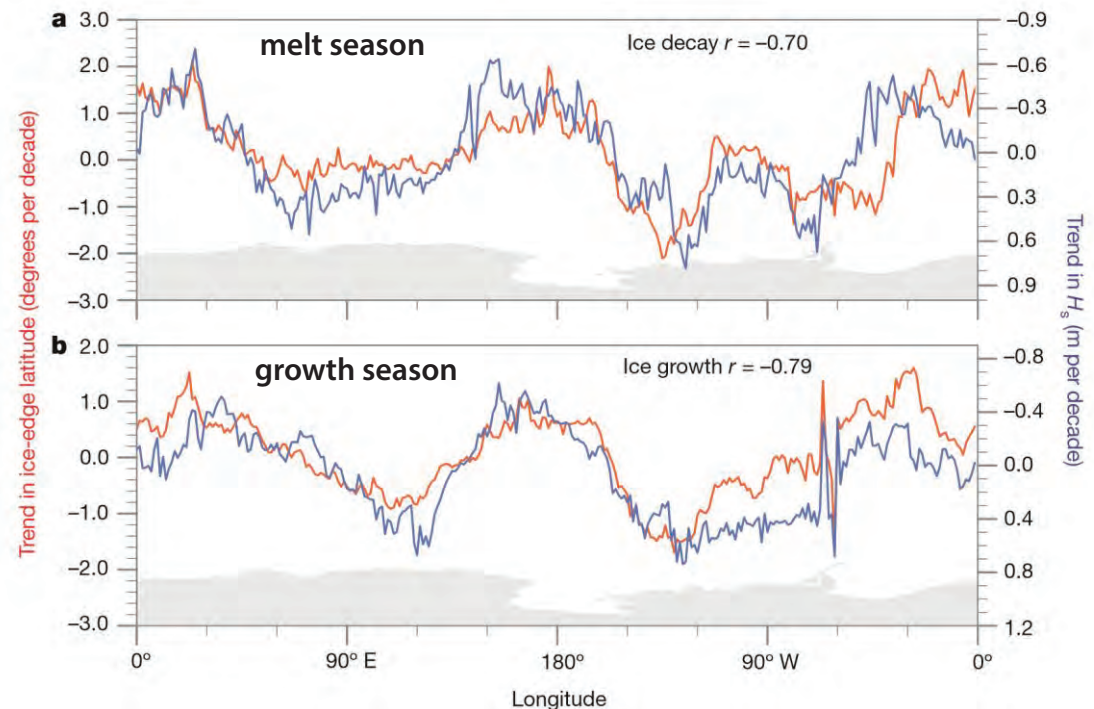


Hardenbrook, Kraitzman, Zhu, Murphy, Cherkaev, Golden

Storm-induced sea-ice breakup and the implications for ice extent

Kohout et al., *Nature* 2014

- during three large-wave events, significant wave heights did not decay exponentially, enabling large waves to persist deep into the pack ice.
- large waves break sea ice much farther from the ice edge than would be predicted by the commonly assumed exponential decay

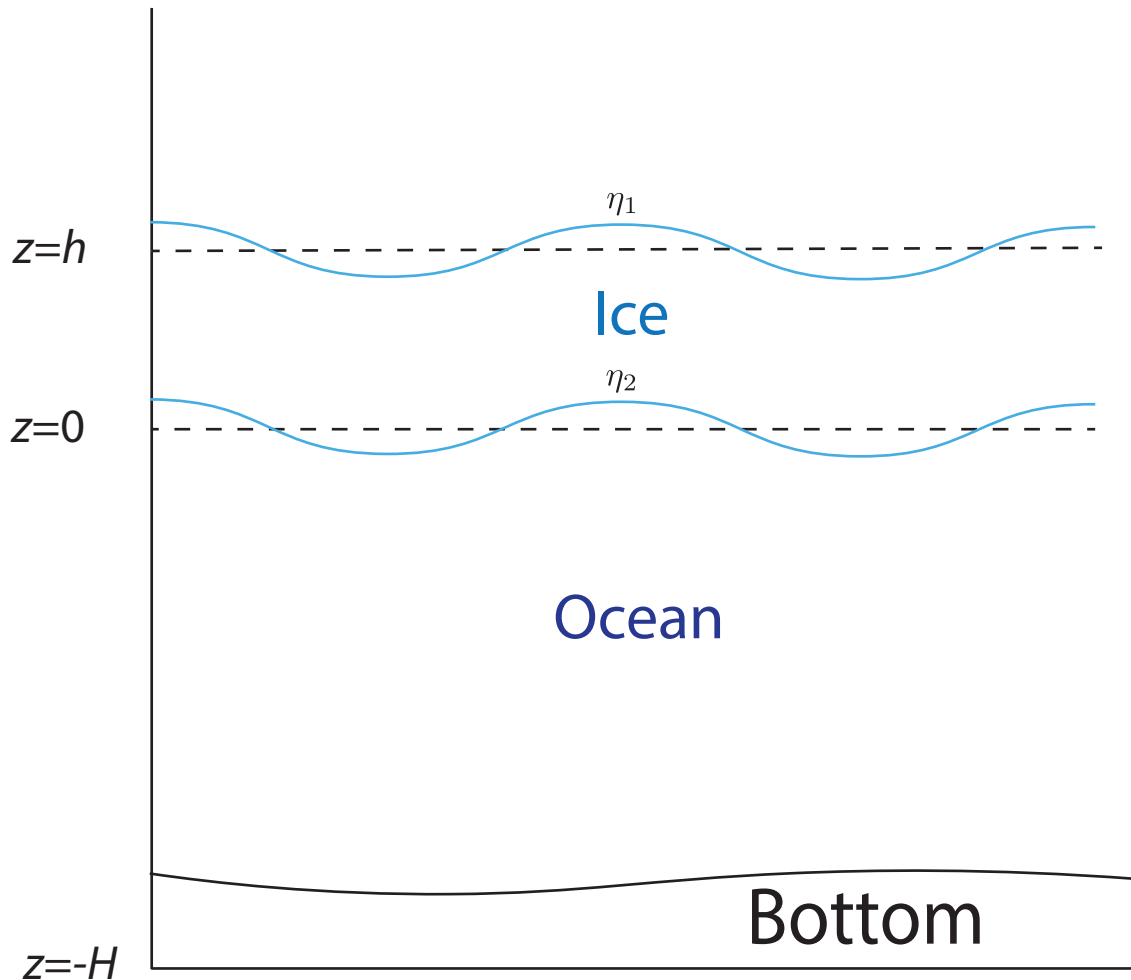


ice extent compared with significant wave height

Waves have strong influence on both the floe size distribution and ice extent.

- 1950 M. L. Weitz and J. B. Keller, *Comm. Pure Appl. Math.*
Reflection of waves from floating ice in water of finite depth
- 1953 M. L. Weitz and J. B. Keller, *Comm. Pure Appl. Math.*
Reflection and transmission coefficients for water waves
entering or leaving an ice field
- 1953 E. Goldstein and J. B. Keller, *EOS Trans. AGU*
Water wave reflection due to surface tension and floating ice
- 1959 F. Karal and J. B. Keller, *J. Acoustical. Soc. Amer.*
Elastic wave propagation in homogeneous and inhomogeneous media
- 1984 K. C. Nunan and J. B. Keller, *J. Fluid Mech.*
Effective viscosity of a periodic suspension
- 1998 J. B. Keller, *J. Geophys. Res. (Oceans)*
Gravity waves on ice-covered water

Two Layer Models and Effective Parameters



Viscous fluid layer (Keller 1998)

Effective Viscosity ν

Equations of motion:
$$\frac{\partial U}{\partial t} = -\frac{1}{\rho} \nabla P + \nu \nabla^2 U + g$$

Viscoelastic fluid layer (Wang-Shen 2010)

Effective Complex Viscosity $\nu_e = \nu + iG/\rho\omega$

Equations of motion
$$\frac{\partial U}{\partial t} = -\frac{1}{\rho} \nabla P + \nu_e \nabla^2 U + g$$

Viscoelastic thin beam (Mosig *et al.* 2015)

Effective Complex Shear Modulus $G_v = G - i\omega\rho\nu$

G shear modulus P pressure ω angular frequency U velocity field
 ν viscosity λ Poisson ratio ρ density g gravity

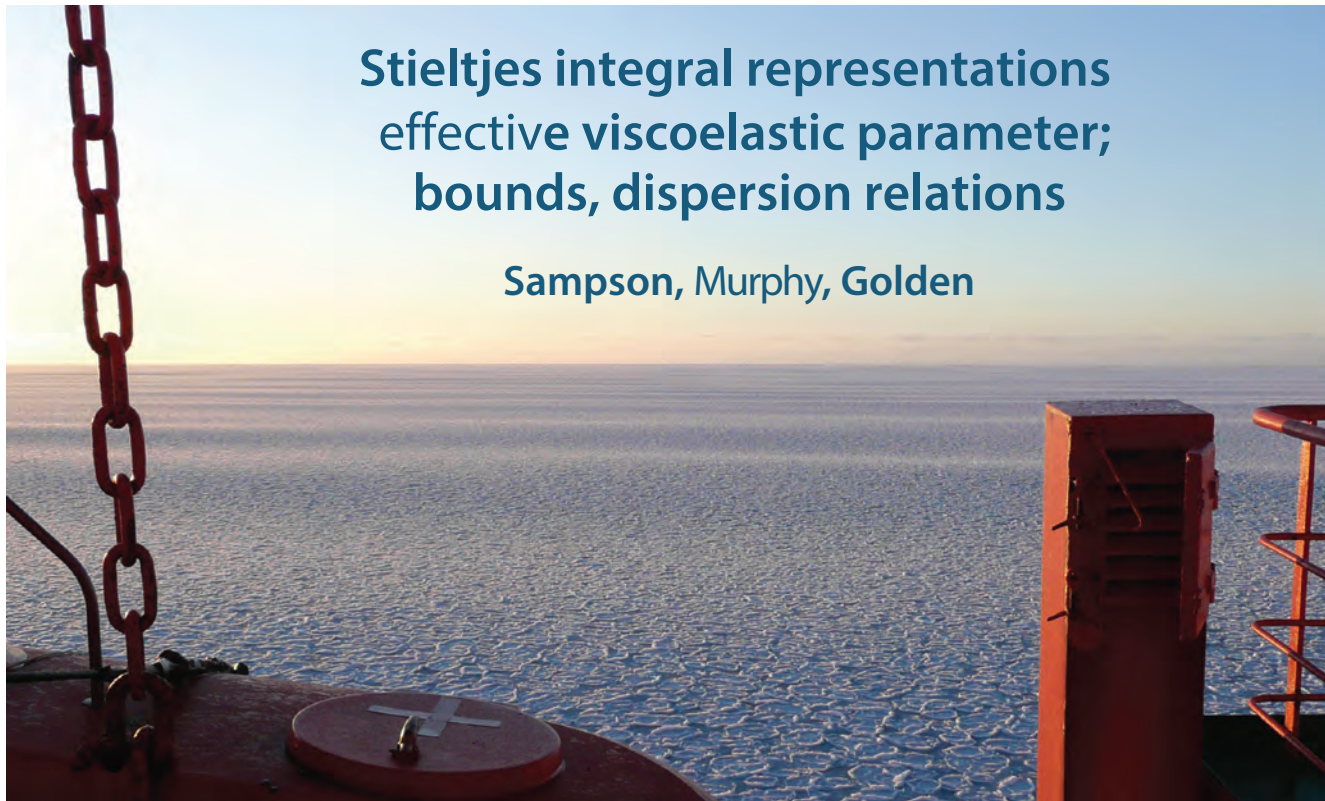
**Stieltjes integral representation
for effective complex viscoelastic
parameter; bounds**

Sampson, Murphy, Golden 2017

wave propagation in the marginal ice zone

Stieltjes integral representations
effective viscoelastic parameter;
bounds, dispersion relations

Sampson, Murphy, Golden



Homogenization Problem for Quasistatic Waves

$$\nabla \cdot \sigma = 0 \quad \sigma = C_{ijkl} : \epsilon_{kl} \quad \langle \sigma \rangle = C_{ijkl}^* \langle \epsilon_{kl} \rangle \quad \text{Strain Field}$$

local $C_{ijkl} = (v_1 \chi + (1 - \chi) v_2) \lambda_s$ $\epsilon = \frac{1}{2} [\nabla u + (\nabla u)^T] = \nabla^s u$

$$\nabla \cdot ((v_1 \chi + (1 - \chi) v_2) \lambda_s : \epsilon) = 0 \quad \epsilon = \epsilon_0 + \epsilon_f \text{ where } \epsilon_f = \nabla^s \phi$$

$$s = \frac{1}{1 - \frac{v_1}{v_2}}$$

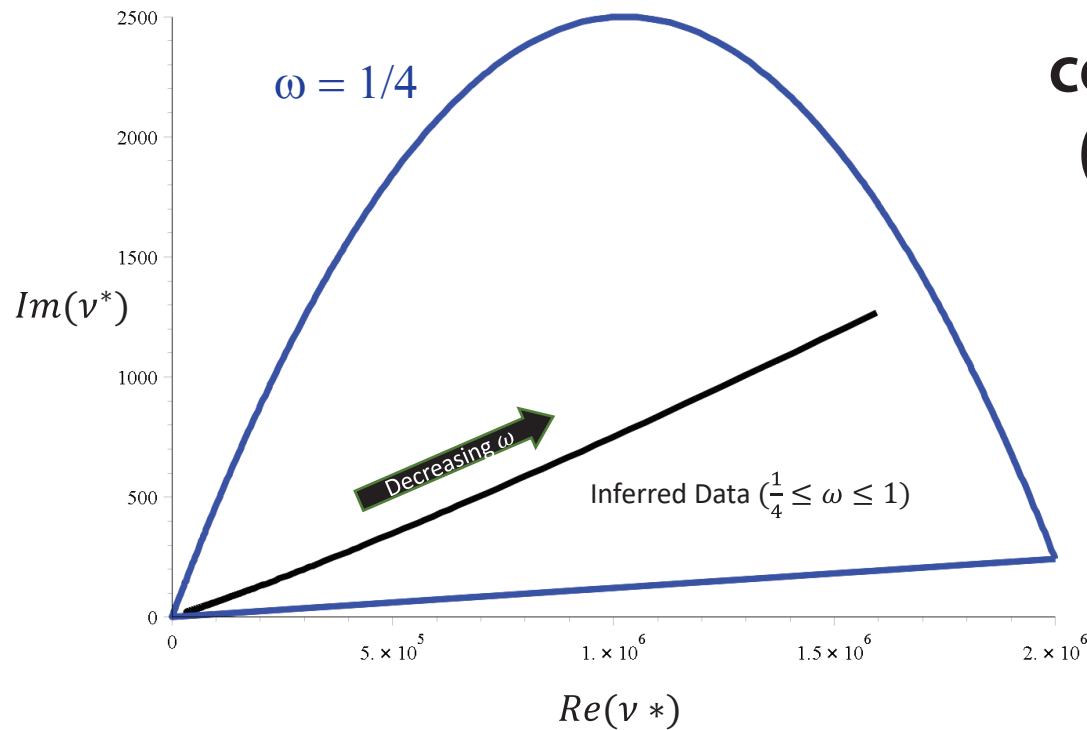
Elasticity Tensor

$$C_{ijkl}^* = v^* \left(\delta_{ik} \delta_{jl} + \delta_{il} \delta_{jk} - \frac{2}{3} \delta_{ij} \delta_{kl} \right) = v^* \lambda_s$$

RESOLVENT $\epsilon = \left(1 - \frac{1}{s} \Gamma \chi \right)^{-1} \epsilon_0 \quad \Gamma = \nabla^s (\nabla \cdot \nabla^s)^{-1} \nabla \cdot \quad \epsilon_0 \text{ avg strain}$

$$F(s) = 1 - \frac{v^*}{v_2} \quad F(s) = ||\epsilon_0||^{-2} \int_{\Sigma} \frac{d\mu(\lambda)}{s - \lambda}$$

bounds on the effective complex viscoelasticity

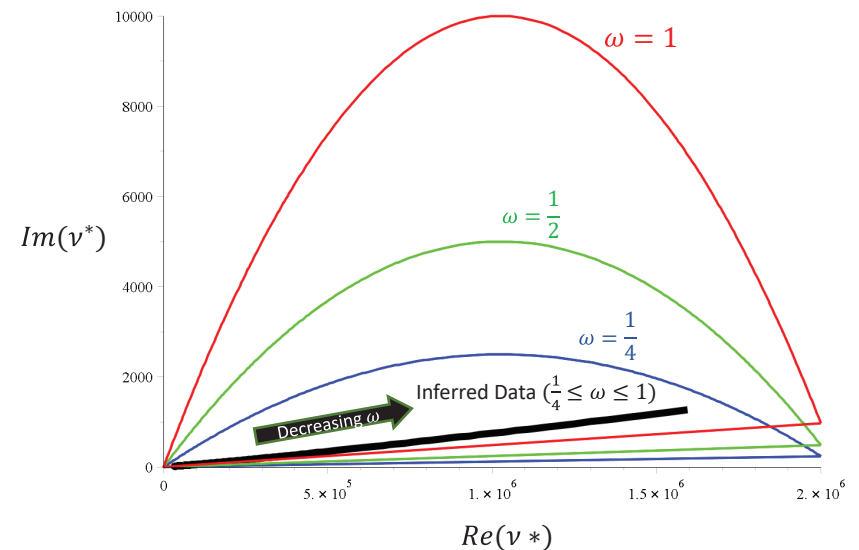


complex elementary bounds
(fixed area fraction of floes)

$$V_1 = 10^7 + i 4875 \quad \text{pancake ice}$$

$$V_2 = 5 + i 0.0975 \quad \text{slush / frazil}$$

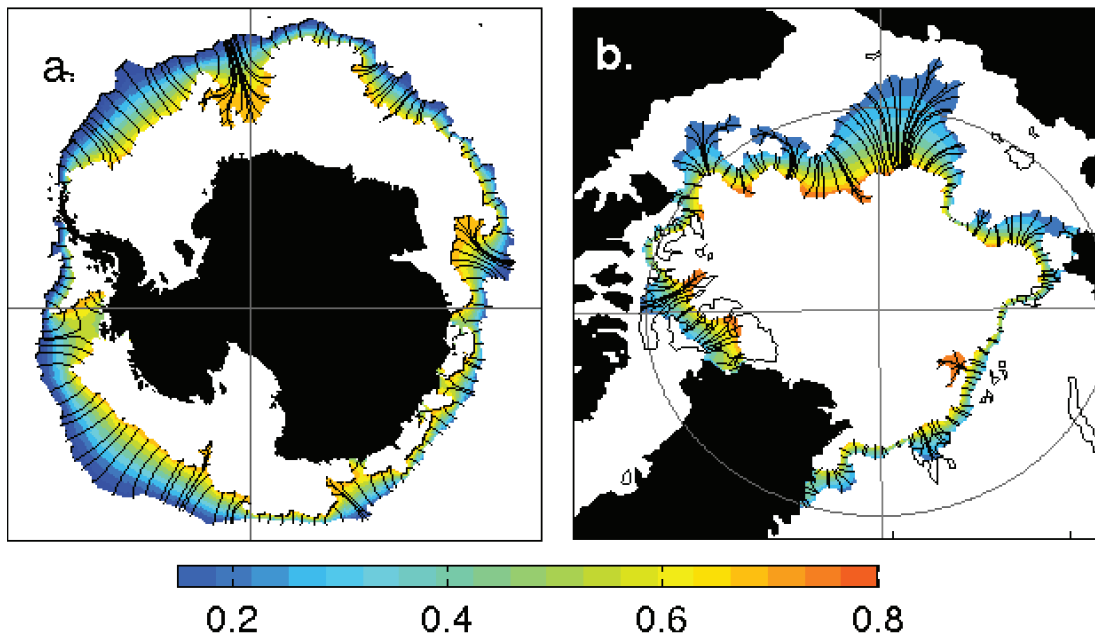
Sampson, Murphy, Golden 2017



Marginal Ice Zone

MIZ

- biologically active region
- intense ocean-sea ice-atmosphere interactions
- region of significant wave-ice interactions



MIZ WIDTH

fundamental length scale of
ecological and climate dynamics

Strong, *Climate Dynamics* 2012

Strong and Rigor, *GRL* 2013

transitional region between
dense interior pack ($c > 80\%$)
sparse outer fringes ($c < 15\%$)

**How to objectively
measure the “width”
of this complex,
non-convex region?**

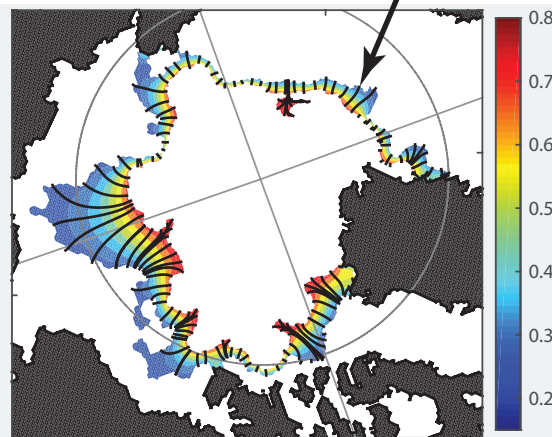
Objective method for measuring MIZ width motivated by medical imaging and diagnostics

Strong, *Climate Dynamics* 2012
Strong and Rigor, *GRL* 2013

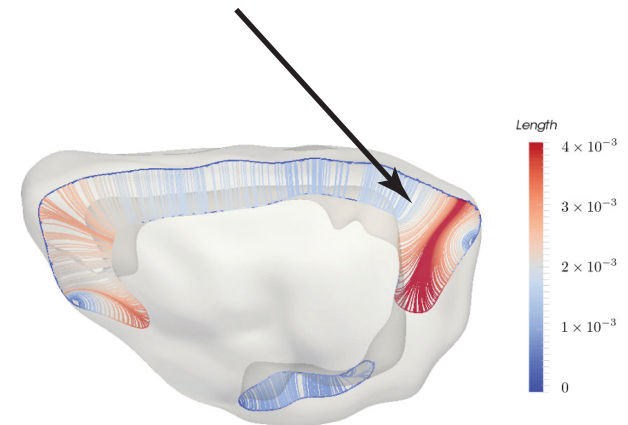
39% widening
1979 - 2012

“average” lengths of streamlines

streamlines of a solution
to Laplace’s equation



Arctic Marginal Ice Zone



**crosssection of the
cerebral cortex of a rodent brain**

analysis of different MIZ WIDTH definitions

Strong, Foster, Cherkaev, Eisenman, Golden
J. Atmos. Oceanic Tech. 2017

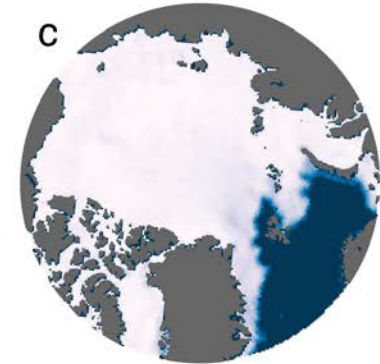
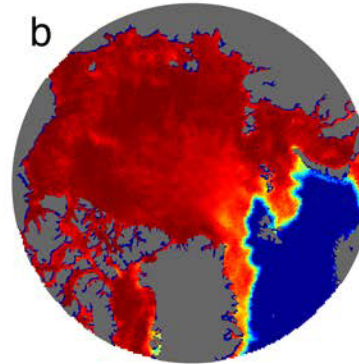
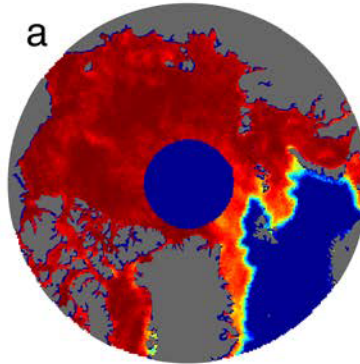
Strong and Golden
Society for Industrial and Applied Mathematics News, April 2017

Filling the polar data gap

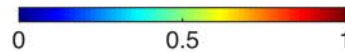
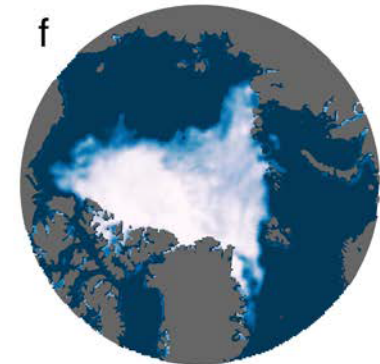
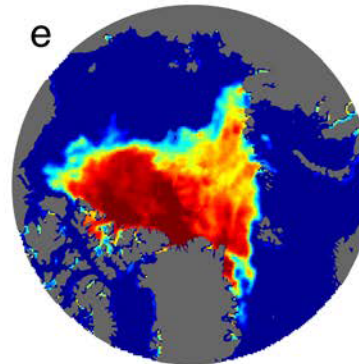
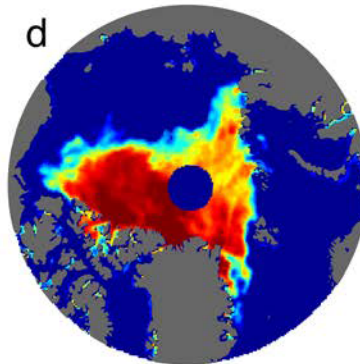
hole in satellite coverage
of sea ice concentration field

previously assumed ice covered

Gap radius: 611 km
06 January 1985



Gap radius: 311 km
30 August 2007



**fill with harmonic function satisfying
satellite BC's plus stochastic term**

Strong and Golden, *Remote Sensing* 2016

Strong and Golden, *SIAM News* 2017

Arctic and Antarctic field experiments

*develop electromagnetic methods
of monitoring fluid transport and
microstructural transitions*

extensive measurements of fluid and
electrical transport properties of sea ice:

2007 Antarctic SIPEX

2010 Antarctic McMurdo Sound

2011 Arctic Barrow AK

2012 Arctic Barrow AK

2012 Antarctic SIPEX II

2013 Arctic Barrow AK

2014 Arctic Chukchi Sea



Notices

of the American Mathematical Society

May 2009

Volume 56, Number 5

Climate Change and
the Mathematics of
Transport in Sea Ice

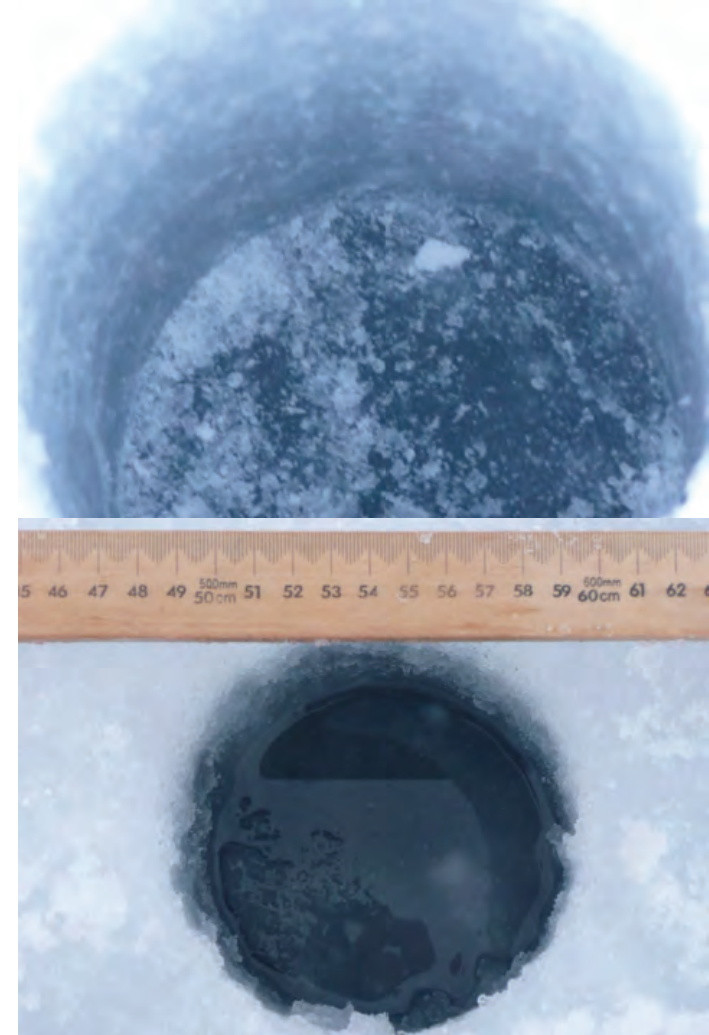
page 562

Mathematics and the
Internet: A Source of
Enormous Confusion
and Great Potential

page 586

photo by Jan Lieser

Real analysis in polar coordinates (see page 613)



***measuring
fluid permeability
of Antarctic sea ice***

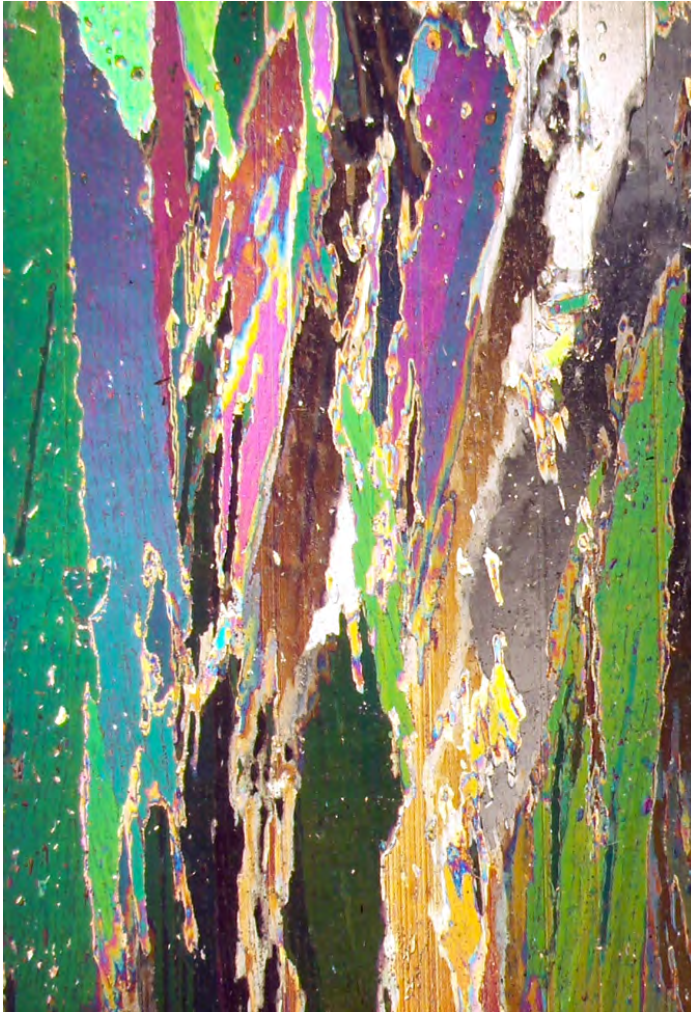
SIPEX 2007

higher threshold for fluid flow in Antarctic granular sea ice

columnar

granular

5%



10%



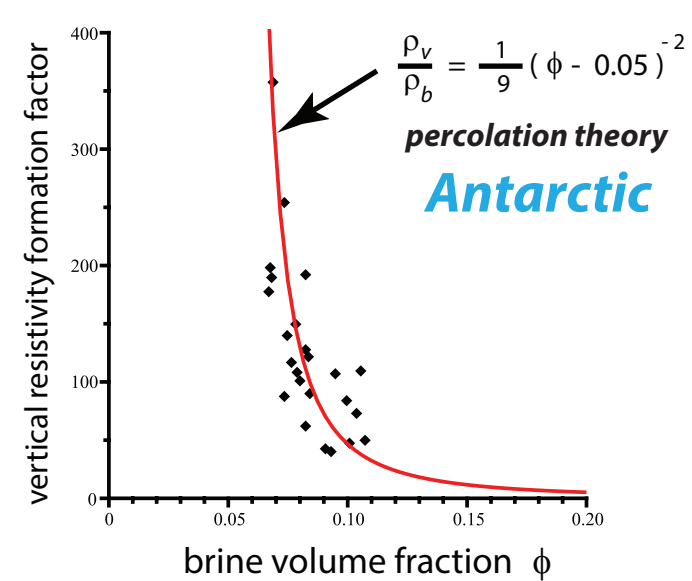
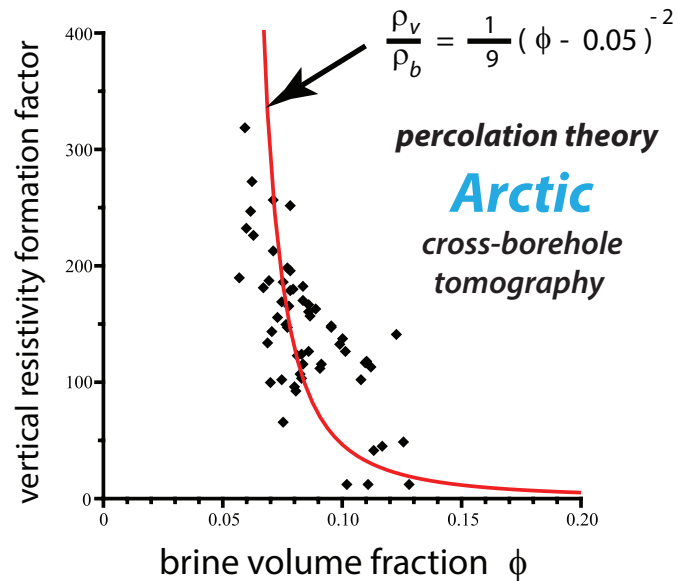
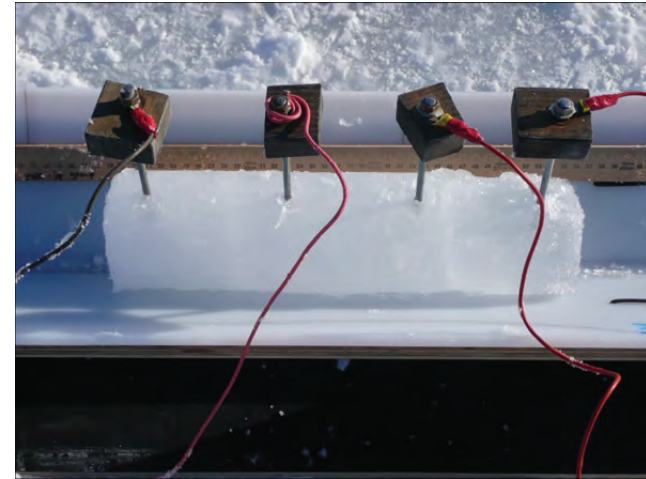
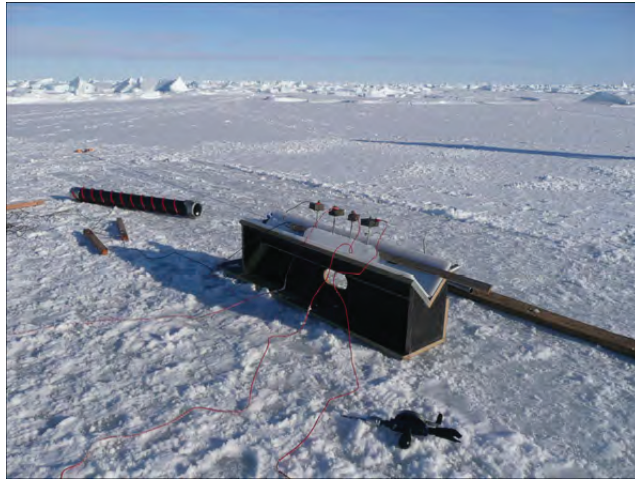
Golden, Sampson, Gully, Lubbers, Tison 2017

tracers flowing through inverted sea ice blocks



critical behavior of electrical transport in sea ice

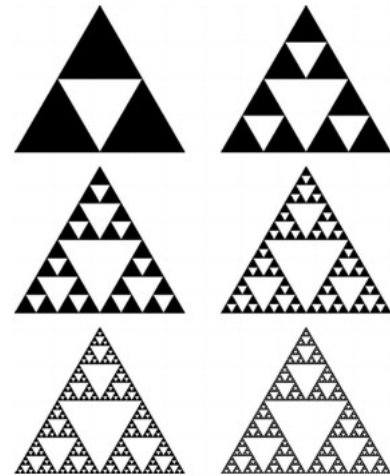
electrical signature of the on-off switch for fluid flow



cross-borehole tomography - electrical classification of sea ice layers

Golden, Eicken, Gully, Ingham, Jones, Lin, Reid, Sampson, Worby 2017

fractals and multiscale structure



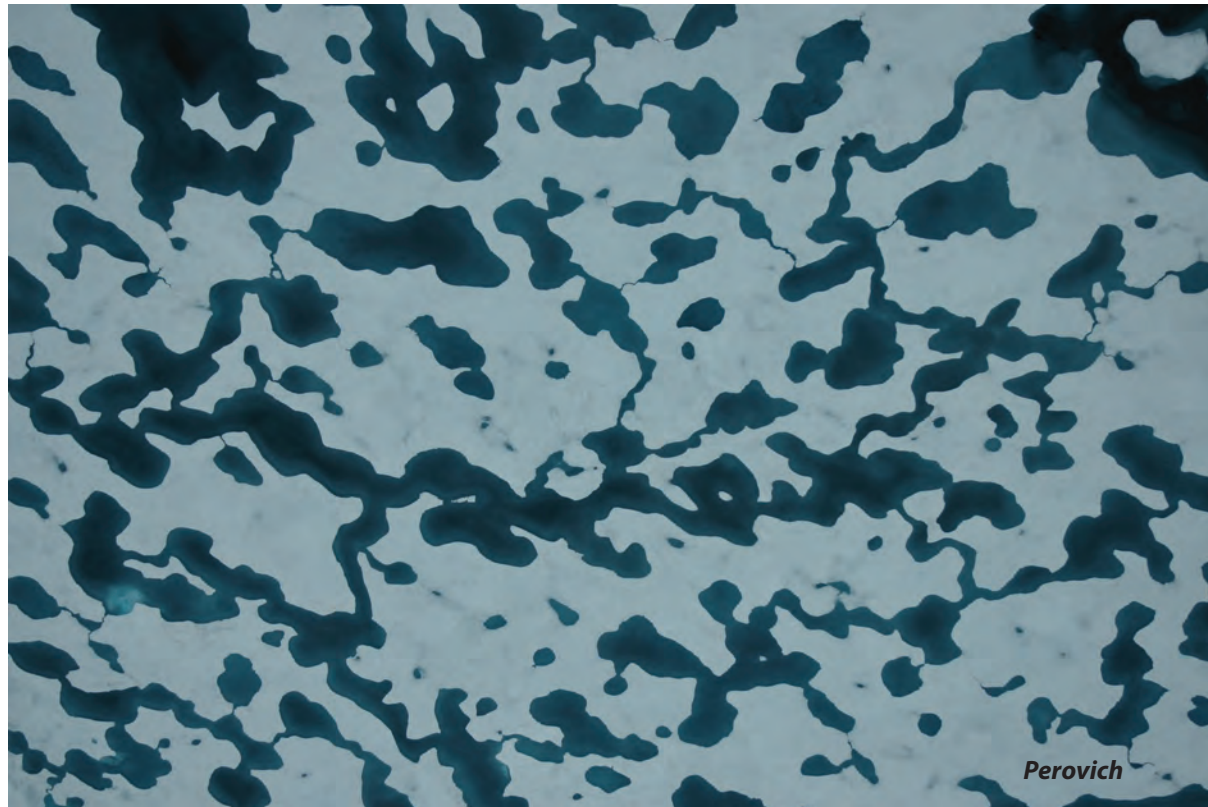
melt pond formation and albedo evolution:

- *major drivers in polar climate*
- *key challenge for global climate models*

numerical models of melt pond evolution, including topography, drainage (permeability), etc.

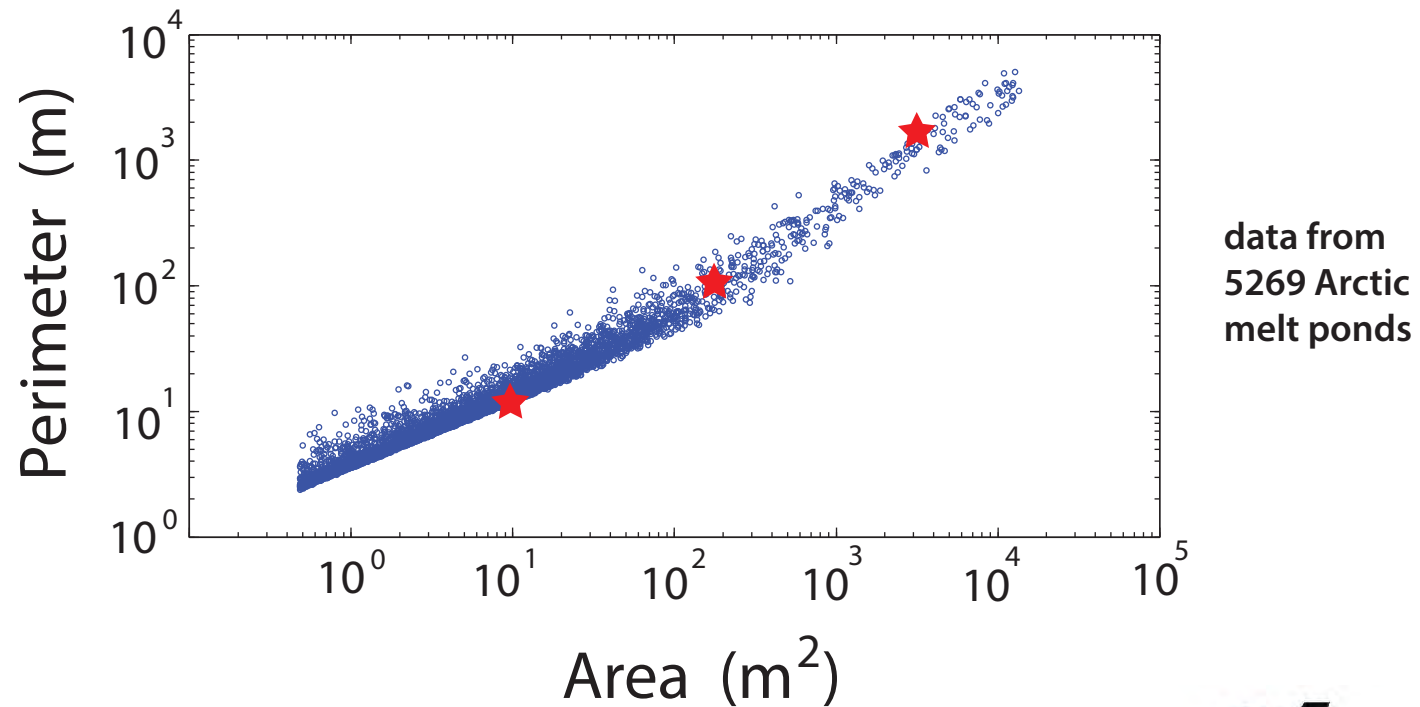
Lüthje, Feltham,
Taylor, Worster 2006
Flocco, Feltham 2007

Skyllingstad, Paulson,
Perovich 2009
Flocco, Feltham,
Hunke 2012



Are there universal features of the evolution similar to phase transitions in statistical physics?

Christel Hohenegger, Bacim Alali, Kyle Steffen, Don Perovich, Ken Golden



simple pond



~ 30 m

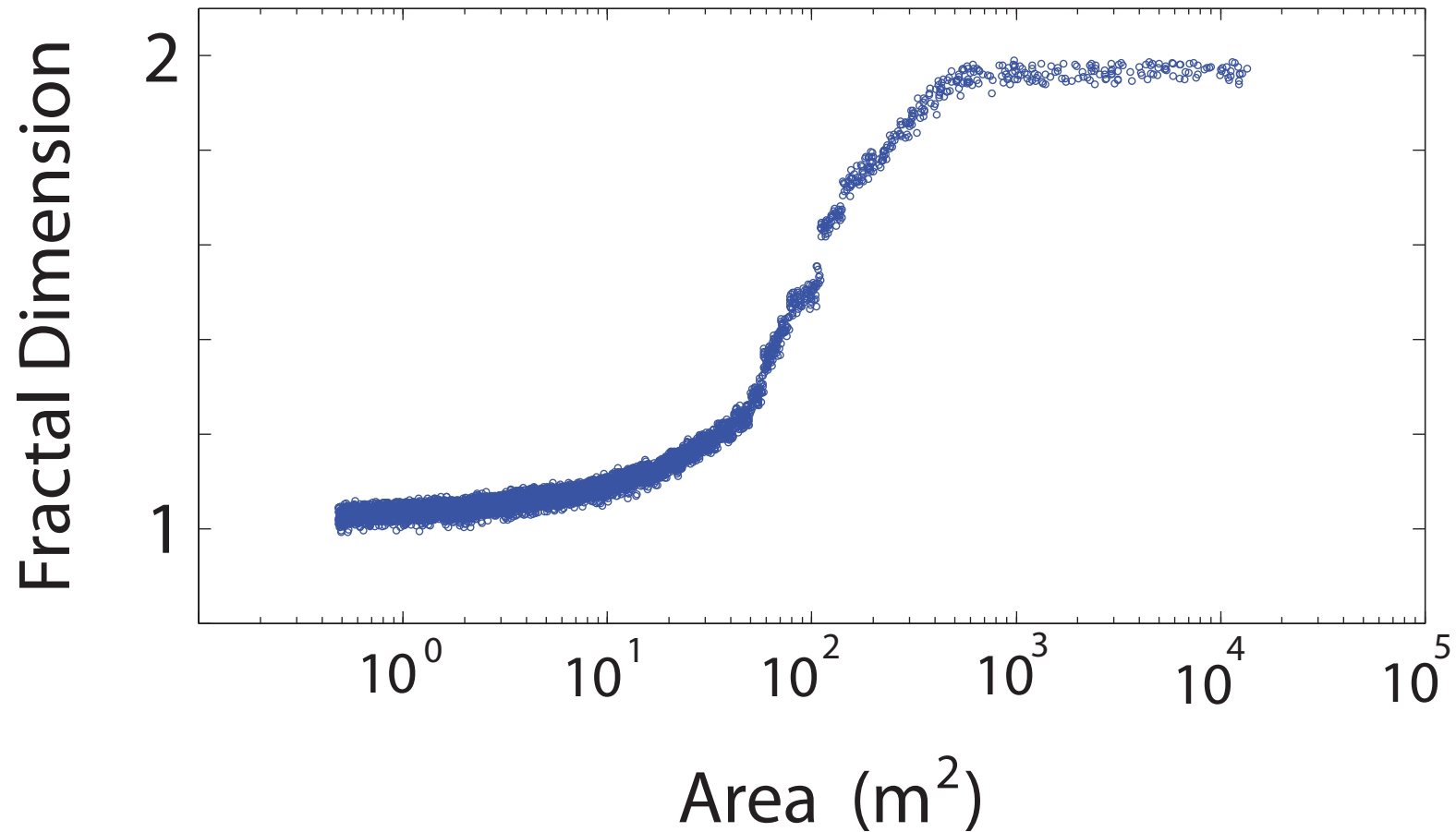
transitional pond



complex pond

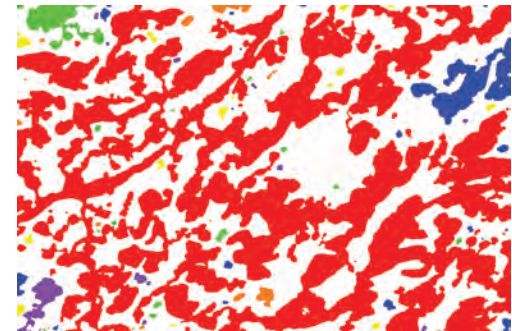
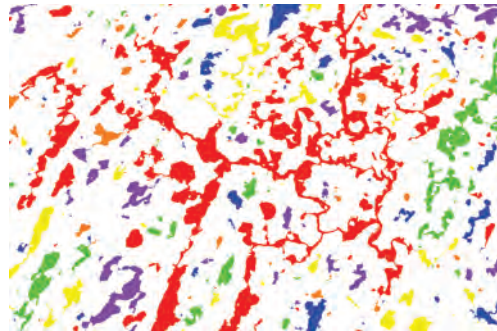
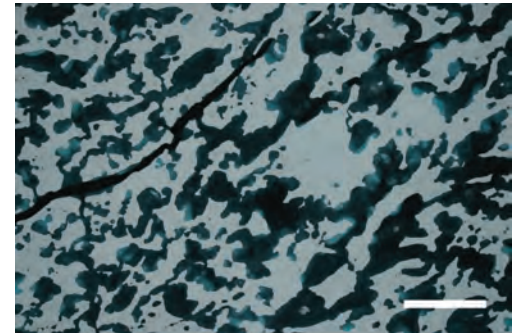
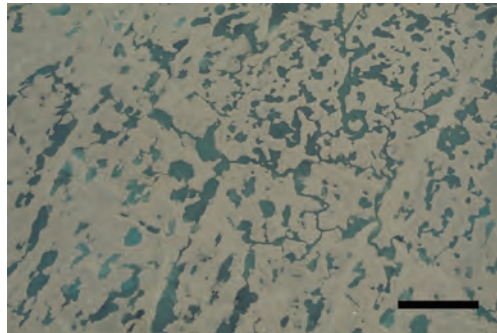
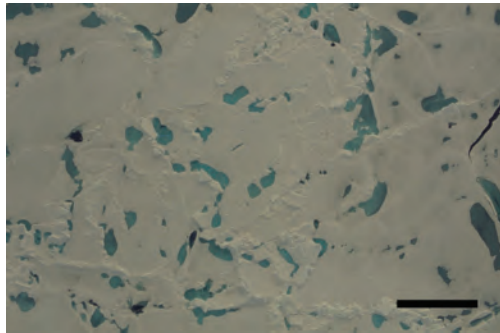
transition in the fractal dimension

complexity grows with length scale



compute “derivative” of area - perimeter data

***small simple ponds coalesce to form
large connected structures with complex boundaries***



melt pond percolation

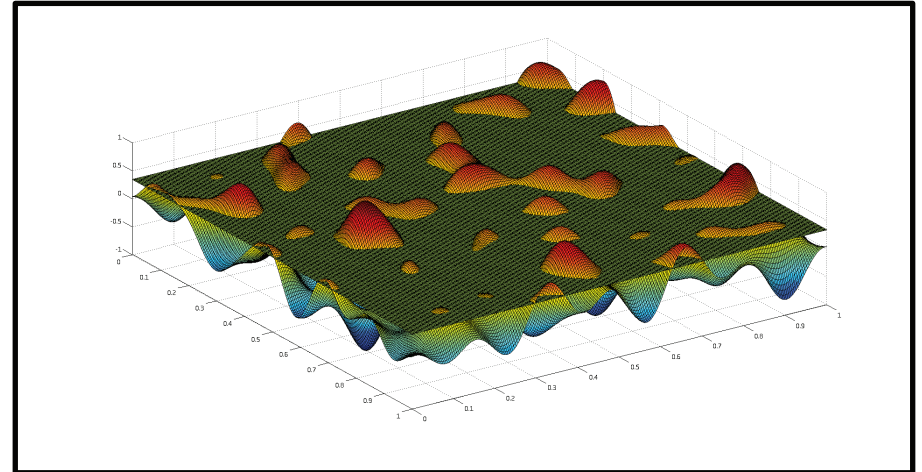
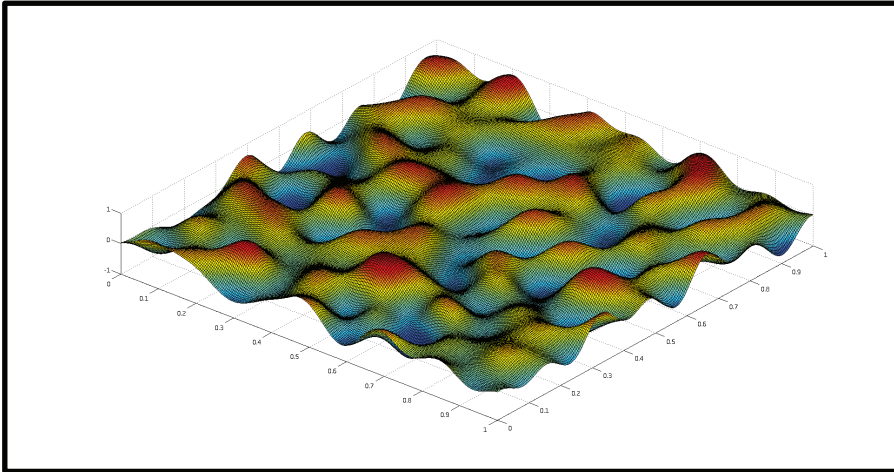
results on percolation threshold, correlation length, cluster behavior

Anthony Cheng (Hillcrest HS), Dylan Webb (Skyline HS), Court Strong, Ken Golden

Continuum percolation model for melt pond evolution

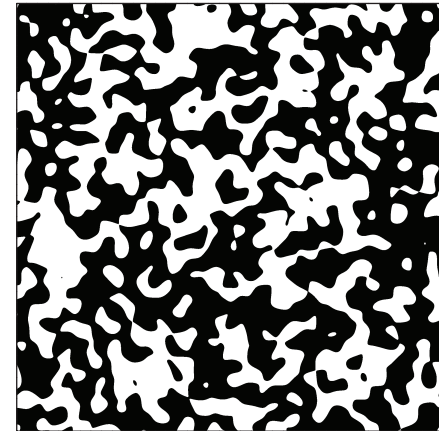
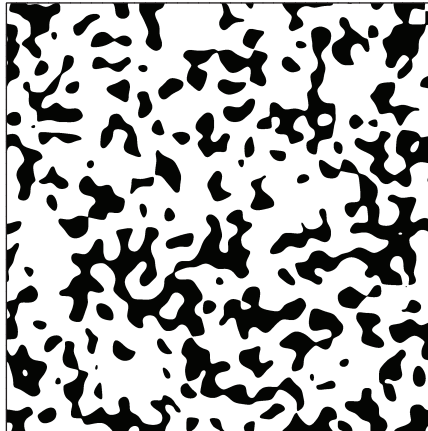
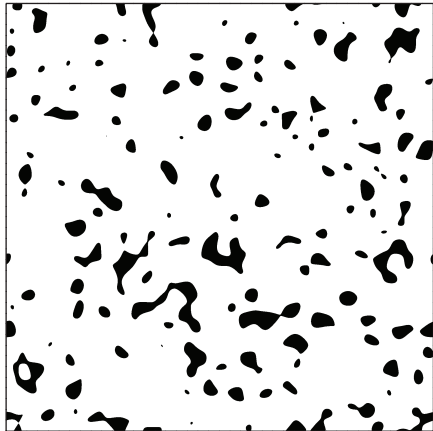
level sets of random surfaces

Brady Bowen, Court Strong, Ken Golden, J. Fractal Geometry 2017



random Fourier series representation of surface topography

intersections of a plane with the surface define melt ponds



electronic transport in disordered media

diffusion in turbulent plasmas

Isichenko, Rev. Mod. Phys., 1992

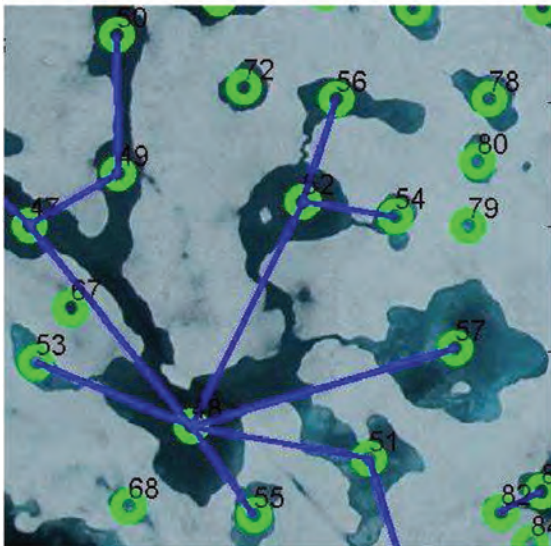
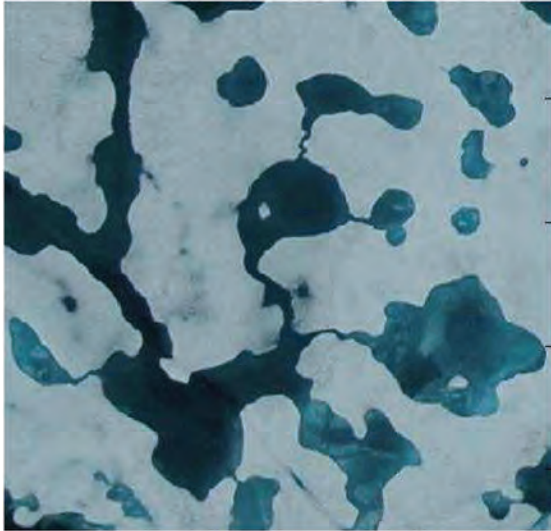
melt pond evolution depends also on large-scale “pores” in ice cover



Melt pond connectivity enables vast expanses of melt water to drain down seal holes, thaw holes, and leads in the ice.

Network modeling of Arctic melt ponds

Barjatia, Tasdizen, Song, Sampson, Golden
Cold Regions Science and Tecnology, 2016



**develop algorithms to map
images of melt ponds onto**

random resistor networks

**graphs of nodes and edges
with edge conductances**

edge conductance \sim neck width

***compute effective
horizontal fluid conductivity***

Ising model for ferromagnets



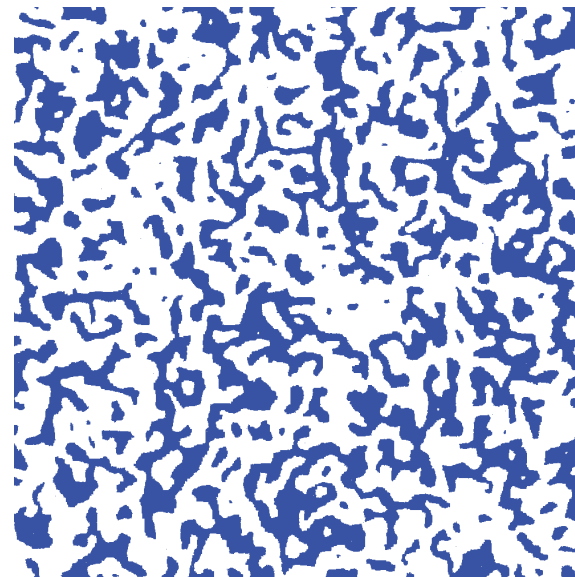
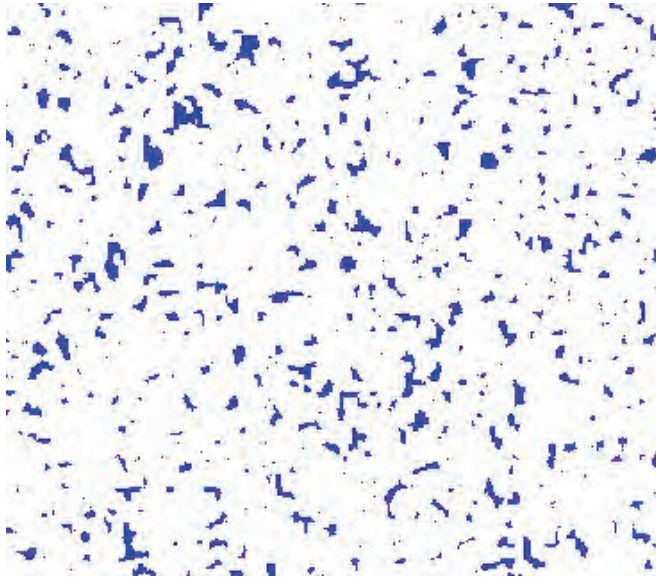
Ising model for melt ponds

$$\mathcal{H}_\omega = -J \sum_{\langle i,j \rangle}^N s_i s_j - H \sum_i^N s_i$$

$$s_i = \begin{cases} \uparrow & +1 & \text{water} & (\text{spin up}) \\ \downarrow & -1 & \text{ice} & (\text{spin down}) \end{cases}$$

magnetization $M = \lim_{N \rightarrow \infty} \frac{1}{N} \left\langle \sum_j s_j \right\rangle$

pond coverage $\frac{(M+1)}{2}$



“melt ponds” are clusters of magnetic spins that align with the applied field

predictions of fractal transition, pond size exponent Ma, Sudakov, Strong, Golden 2017



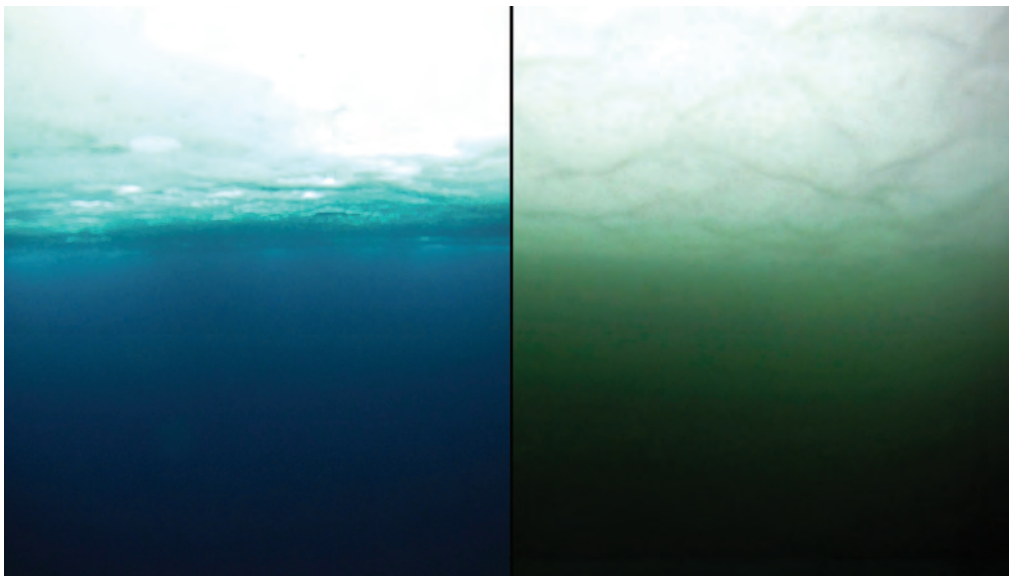
2011 massive under-ice **algal bloom**

Arrigo et al., *Science* 2012

melt ponds act as

WINDOWS

allowing light
through sea ice



no bloom

bloom

***Have we crossed into a
new ecological regime?***

The Melt Pond Conundrum:

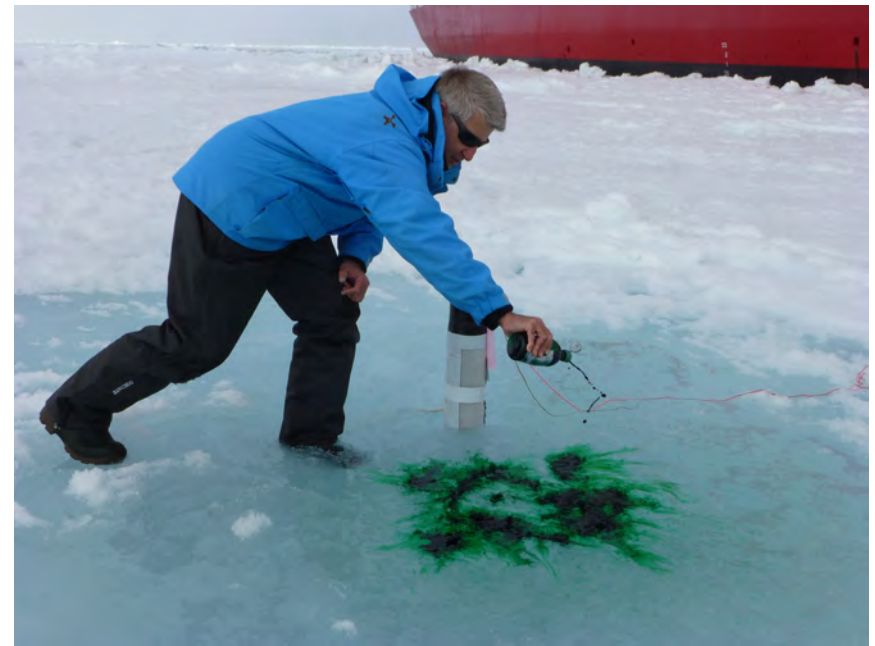
How can ponds form on top of sea ice that is highly permeable?

C. Polashenski, K. M. Golden, D. K. Perovich, E. Skyllingstad, A. Arnsten, C. Stwertka, N. Wright

Percolation Blockage: A Process that Enables Melt Pond Formation on First Year Arctic Sea Ice

J. Geophys. Res. Oceans 2017

*2014 Study of Under Ice Blooms in the Chuckchi Ecosystem (SUBICE)
aboard USCGC Healy*



Conclusions

1. Summer Arctic sea ice is **melting rapidly**, and **melt ponds** and other processes must be accounted for in order to predict melting rates.
2. **Fluid flow** through sea ice mediates **melt pond evolution** and many processes important to climate change and polar ecosystems.
3. **Statistical physics and homogenization help link scales**, provide rigorous methods for finding effective behavior, and advance how sea ice is represented in climate models.
4. Critical behavior (in many forms) is inherent in the climate system.
5. Field experiments are essential to developing relevant mathematics.
6. Our research will help to **improve projections of climate change**, the fate of Earth's sea ice packs, and the ecosystems they support.

Joe Keller had a broad impact on the math we use to model sea ice...

THANK YOU

National Science Foundation

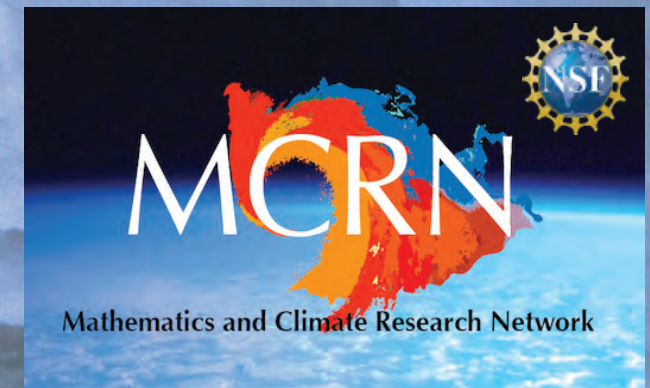
Division of Mathematical Sciences

Division of Polar Programs

Office of Naval Research

Arctic and Global Prediction Program

Applied and Computational Analysis Program



Buchanan Bay, Antarctica Mertz Glacier Polynya Experiment July 1999